Gonçalo Miguel Rodrigues de Brito Barros

Licenciado em Ciências da Engenharia Electrotécnica
e de Computadores

Serviços Pós-4G em Redes de Satélite LEO com Recepção Multi-Pacote e com Handover

Dissertação para obtenção do Grau de Mestre em
Engenharia Electrotécnica e de Computadores

Orientadores : Luís Bernardo, Professor Auxiliar, FCT-UNL
Rui Dinis, Professor Auxiliar com Agregação, FCT-UNL

Júri:

Presidente:	Prof. Paulo Montezuma
Arguente:	Prof. António Rodrigues
Vogais:	Prof. Luís Bernardo
	Prof. Rui Dinis

FACULDADE DE
CIÊNCIAS E TECNOLOGIA
UNIVERSIDADE NOVA DE LISBOA

Setembro, 2012

Serviços Pós-4G em Redes de Satélite LEO com Recepção Multi-Pacote e com Handover

Acknowledgements

First of all i would like to thank to my supervisor Prof. Luís Bernardo for giving me the opportunity to realize this dissertation. His knowledge, availability and patience were extremely important during all the time i spent doing this work. I am also grateful to my co-supervisor Prof. Rui Dinis and to Prof. Paulo Montezuma, who were truly fundamental in my dissertation development.

I am very thankful to UNINOVA for giving me the chance to participate in the project MPSAT PTDC/EEATEL/099074/2008, and for providing me a research grant during four months.

It would not be possible for me to reach this stage without my course colleagues. I am specially grateful to João Melo, Francisco Esteves, Gonçalo Alves, Nuno Vasconcelos, António Furtado, João Rodrigues and Gonçalo Carvalho, for their friendship, and for all the time they spent helping me when i needed.

I am totally blessed for having Ana Roque as my girlfriend. She was always by my side during all the course, and beyond the love and the friendship, she always believed in my capabilities and in my will to succeed.

I'm very lucky to have amazing friends outside the faculty. I would like to thank specially to Pedro Amaro, Paulo Borges, Tiago Nascimento, Isaque Tito, Mauro Alves and David Gaspar, for all the moments of joy, and for the proofs of real friendship that you daily show to me since we were little boys. I could not write my acknowledgements without mentioning my big friend Emanuel Neto, that will not read this, but his advices and all the things that he taught me, will always be present in my life.

Last but not least, i want to thank to my parents Luís and Maria da Luz for everything that they gave me and still give. I can not describe what they mean to me in words, neither the effort that they made to raise me as good as possible. I am totally grateful to my grandmothers Maria Antónia and Emília for their importance in my life, and for showing me the most important values that a man should have.

Abstract

Traditionally, a packet with errors, either due to channel noise or collisions, is discarded and needs to be retransmitted, leading to performance losses. Hybrid Automatic Retransmission reQuest (H-ARQ) and time diversity multipacket reception approaches, such as Network Diversity Multiple Access (NDMA), improve the system performance by requesting additional retransmissions and combining all the signals received together. However, the high round trip delay time associated to satellite networks introduces limitations in the number of retransmission requests that may be issued by the terminals to fulfil the Quality of Service (QoS) requirements.

This thesis considers the design of hybrid protocols combining H-ARQ and NDMA for satellite networks with demand-assigned traffic. The satellite NDMA (S-NDMA) protocol is presented and analytical models are proposed for its performance. Energy efficient QoS provisioning is also analysed. The proposed system's performance is evaluated for a Low Earth Orbit (LEO) network with a Single-Carrier with Frequency Domain Equalization (SC-FDE) scheme, and compared to H-NDMA. Results show that the proposed system is energy efficient and can provide enough QoS to support high demand services such as video telephony.

Several satellites are needed to cover a broad area of the planet. As the satellites are constantly moving, their footprints are permanently changing positions. This leads to a need for a handheld mobile terminal to change its communication to another satellite. Two handover schemes are proposed on this thesis for S-NDMA protocol: the conventional cold handover and an hot handover based on a distributed Single-Input Multiple-Output (SIMO) approach. Their feasibility and performance are compared, taking into account the energy efficiency, the Doppler deviation, the optimal handover point and time offset.

Keywords: S-NDMA, H-NDMA, SC-FDE, Satellites, Doppler deviation, Quality of Service

Resumo

Um pacote com erros, quer seja devido à existência de colisões ou ruído no canal, é normalmente descartado e necessita de ser retransmitido, levando a perdas de desempenho. A junção do protocolo H-ARQ (Hybrid Automatic Retransmission reQuest) com técnicas de recepção multi-pacote e com diversidade temporal como o NDMA (Network Diversity Multiple Access), melhoram o desempenho, visto terem a capacidade de pedir transmissões extra e combinar todos os sinais recebidos no mesmo período. Contudo, o atraso provocado pelo tempo de ida e volta na comunicação com uma rede de satélites, limita o número de retransmissões que possam ser pedidas pelos terminais para garantir qualidade de serviço.

Esta tese considera o desenho de um protocolo híbrido que combina H-ARQ com NDMA para redes satélites com tráfego atribuído a pedido. O protocolo S-NDMA (Satellite NDMA) é apresentado, juntamente com modelos analíticos para o seu desempenho. É analisada a sua eficiência energética, tendo em conta requisitos de qualidade de serviço (QoS). O sistema é feito para satélites de órbita baixa (LEO) e com SC-FDE (Single-Carrier with Frequency Domain Equalization). É feita também uma comparação de desempenhos deste esquema com H-NDMA (Hybrid-NDMA), mostrando que é eficiente em termos energéticos e que cumpre requisitos de QoS para serviços exigentes como videochamadas.

São necessários vários satélites para cobrir uma vasta área do planeta. Como os satélites estão em constante movimento, a zona de cobertura associada a cada satélite também se desloca. Isto leva a uma necessidade do terminal móvel trocar constantemente de ligação para um novo satélite. Nesta dissertação são propostos dois esquemas para S-NDMA: o tradicional com interrupção temporária de ligação, e um novo com continuidade de ligação baseado em SIMO distribuído. São estudadas a viabilidade e desempenho dos dois esquemas, analisando-se a eficiência energética, o efeito de Doppler, o ponto óptimo de troca e o atraso no tempo na comunicação entre terminais móveis e satélites.

Palavras-chave: S-NDMA, H-NDMA, SC-FDE, Satélites, Doppler deviation, Qualidade de Serviço

Contents

List of Figures

Acronyms List

3GPP 3rd Generation Partnership Project

ACK Acknowledgement

ARQ Automatic Repeat Request

AWGN Additive White Gaussian Noise

BER Bit Error Rate

BS Base Station

CDMA Code Division Multiple Access

CP Cyclic Prefix

CSMA/CD Carrier Sense Multiple Access with Collision Detection

CSMA Carrier Sense Multiple Access

DAMA Demand Assigned Multiple Access

EFC Earth Fixed Cell

FDE Frequency Domain Equalization

FDM Frequency Division Multiplexing

FDMA Frequency Division Multiple Access

FEC Forward Error Correction

FFT Fast Fourier Transform

FIFO First-In First-Out

GBN Go-Back-N

GSM Global System for Mobile Communications

GSO Geostationary Orbit

H-ARQ Hybrid-Automatic Repeat Request

H-MAC Hybrid-Medium Access Control

H-NDMA Hybrid-ARQ NDMA

IC Interference Cancellation

IFFT Inverse Fast Fourier Transform

IP Internet Protocol

ISI Intersymbol Interference

ISL Inter Satellite Link

KMA Known Modulus Algorithms

LDPC Low Density Parity Check

LEO Low Earth Orbit

LTE Long Term Evolution

MAC Medium Access Control

MEO Medium Earth Orbit

MIMO Multiple-Input Multiple-Output

MMSE Minimum Mean Square Error

MPR Multiple Packet Reception

MUD Multi-User Detection

MT Mobile Terminal

M-QAM Multi-Level Quadrature Amplitude Modulation

NACK Negative Acknowledgement

NDMA Network-assisted Diversity Multiple Access

NGSO Non-Geostationary Orbit

OFDM Orthogonal Frequency Division Multiplexing

OSI Open Systems Interconnection

PAPR Peak average power ratio

PER Packet error rate

PHY Physical

PIC Parallel Interference Cancellation

PSTN public switching telephone network

QoS Quality of Service

QPSK Quadrature Phase Shift Keying

RF Radio Frequency

RSSI Radio Signal Strength Indicator

RTT Round-Trip-Time

SC Single Carrier

SC-FDE Single Carrier - Frequency Domain Equalization

SFC Satellite Fixed Cell

SIC Successively Interference Cancellation

SISO Single-Input Single-Output

SIMO Single-Input Multiple-Output

SMS Short Message Service

S-NDMA Satellite-Network-assisted Diversity Multiple Access

SNR Signal-to-noise ratio

SR Selective Repeat

TC Turbo Codes

TDMA Time Division Multiple Access

UHF Ultra High Frequency

V-BLAST Vertical-Bell Laboratories Layered Space-Time

VHF Very High Frequency

VSAT Very-small-aperture terminal

WLAN Wireless Local Area Network

1

Introduction

1.1 Motivation

The future of telecommunications aims to provide permanent and ubiquitous connectivity, regardless of location. Satellite communication systems can lead telecommunications networks to a level where they provide global connectivity anywhere and any time; they make possible a reachability on inaccessible areas, or areas where terrestrial infrastructure has been damaged. By having a global reach, with a flexible bandwidth-on-demand capability, these networks make possible the access to satellites channels from any earth station within satellite's coverage area[CY99].
The motivation behind this dissertation was *LightSquared technology*, which has the intention to provide 4G wireless broadband services, by combining a worldwide Long Term Evolution (LTE) terrestrial network with ubiquitous satellite coverage. This combination between terrestrial and satellite technology provides an user ubiquitous connectivity.
Compared to terrestrial cellular infrastructures, satellite networks have higher propagation delays and require much higher transmission power due to the large distance between the terminal and the satellite. Although, satellite networks complement the terrestrial cellular infrastructure, supporting ubiquitous data and multimedia services with guaranteed Quality of Service (QoS). To be effective, the Mobile Terminals (MTs) must have low cost and operate with low power. Therefore, energy efficiency is a major requirement for such systems.

1.2 Objectives and Contributions

A Low Earth Orbit (LEO) satellite network with a SC-FDE scheme is considered on this dissertation. The satellite network considered, is based in *Iridium* satellite constellation [www10], so characteristics of this Motorola's system are present throughout the dissertation chapters. This research work took into account the recently proposed Hybrid-ARQ NDMA (H-NDMA) [GPB+11], which was created to enhance NDMA [TZB98] protocol's error resilience capability. However, H-NDMA is unsuitable for satellite networks due to the multiple control packets required for additional retransmissions and acknowledgements, which may introduce delay and jitter incompatible with several kinds of QoS requirements [AMCV06]. So, in order to overlap those issues, a S-NDMA protocol is proposed in this dissertation.

S-NDMA adapts the design of H-NDMA principles to a Demand Assigned Multiple Access (DAMA) satellite scenario, adapting Hybrid-Automatic Repeat Request (H-ARQ) to work with a bounded number of acknowledgement packets. The first part of this contribution is present in chapter 3, where S-NDMA is presented and analytical models are proposed for obtaining the throughput, energy consumption and transmission delay of S-NDMA. In another relevant original contribution, this dissertation defines an optimization approach for S-NDMA to minimize the energy consumption satisfying a set of QoS requirements on a DAMA scenario, where the number of MTs (Mobile Terminals) transmitting is known *a priori*. Those QoS requirements were chosen to match the rigorous requirements of services like video streaming or video telephony applications. S-NDMA is compared with H-NDMA protocol on chapter 3, in order to clarify the performance differences between both protocols.

As the LEO satellites are constantly moving around the planet, their footprints move synchronously with them. So, in order to maintain constant connectivity, it is necessary for an handheld Mobile Terminal (MT) to communicate with more than one satellite at the same time, while it is constantly switching its connection to a new satellite. This dissertation contributes with the design of a soft handover approach based on a distributed Single-Input Multiple-Output (SIMO) approach. This new handover approaches performance is analysed for two different satellite constellations with different handover schemes for S-NDMA protocol: an intra-planar handover scheme and another one based on *Iridium* satellite constellation [www10]. Chapter 4 explains in detail the design of the soft handover approach, and presents the consequences of communicating with more than one satellite in terms of throughput, energy consumption and transmission delay. As the movement of satellite is considered on chapter 4, it brings issues like Doppler effect and offset on time, which are also approached on chapter 4. One paper was published [ICCCN12] and a second one was submitted to the conference IEEE VTC 2013 spring in result of the work developed in this dissertation.

1.3 Dissertation structure

The dissertation structure is briefly organized as follows: Chapter 2 contains related work overview that was essential to develop this dissertation; Chapter 3 presents the S-NDMA protocol proposal and its comparison with H-NDMA protocol, as well as performance results in terms of energy, transmission delay and throughput; Chapter 4 contains the proposed handover scheme, and analysis its performance in energy consumption, transmission delay, throughput, time offset and Doppler deviation; The last chapter 5 contains the conclusions and also incorporates future work that could be done by taking this dissertation as a reference.

2

Literature Review

2.1 Satellite Constellations

It is important to know about satellite constellations and subsequent orbit types before developing satellite networks.
There are two main known types of satellite constellations: Geostationary Orbit (GSO) and Non-Geostationary Orbit (NGSO)[CAI06a][BWZ00].
In the first case, satellites move circularly around the Earth in approximately twenty four hours, which means that they move synchronously with the planet movement. GSO constellation stands in equator plane at an altitude of 35786 Km. As the altitude for Earth's surface is large, each satellite covers one third of the planet, so there is no need to have a large number of satellites to cover the entire Earth's surface.
The big altitude in GSO constellations could have a counterpoint in terms of power consumption from MTs and propagation delay, which is too high for real time applications. Inmarsat satellite system is an example of a GSO constellation.
In Non-Geostationary constellations, the satellites movement is asynchronous in relation to Earth's movement. NGSO could be Low Earth Orbit (LEO) where satellites stand above the Earth's surface at an altitude between 500 and 2000 km, or Medium Earth Orbit (MEO), which have satellites at an altitude of 3000 to 4000 km. Both orbits can be circular or elliptical. A disadvantage of NGSO in relation to GSO constellations is the lower Earth's surface coverage due to the minor altitude where satellites are standing. However, an advantage of NGSO constellations over GSO constellations is the lower propagation delay, allowing the usage of real time applications.
Examples of NGSO constellations for mobile satellite systems are GlobalStar, Iridium or ICO constellations [AM96].

2.2 Satellite System Architecture

Several parameters must be taken into account in the design of a LEO satellite constellation, including transmission delay, service coverage, minimum elevation angle and the effects of space radiation [SY07]. A satellite system can be presented as an access network or as a core network.
In the first case, the satellite retransmits the signal that is received from a terminal to a gateway on earth. This gateway transmits the signal to a terrestrial core network, where the transmission to further neighbours is proceeded.
Regarding the latter case, which is the access/core network, the satellite receives the signal from the terminal and passes it through Inter Satellite Link (ISL) (which are part of a satellite network), until the satellite that serves the destination terminal is reached. These Inter Satellite Link (ISL), can be established between satellites belonging to the same type of orbit, and a link-budget is provided for the link connected to the terminal. Initially, satellites worked as retransmission stations, so the regeneration of the signal was not implemented on them.
In the first satellite systems the retransmission between satellites was made in a transparent way, which means that it is not adapted to a defined protocol type, so the signal could only be modified on Earth. This had some advantages, in view of bandwidth occupied by the transmitted signal that was not reduced. The link budget on Earth-to-satellite and vice-versa connections, due to the non-regeneration of the signal on the satellites, has a joint effect, which affects the emitted power and the size of antennas.
The processing and switching methods have been improved in more recent systems, so each satellite can have steerable multi-beam antenna, allowing the track of user terminals through digital beam-forming.
The ISL network is controlled by on-board routing functions of the satellites [SY07][BWZ00]. In this case, terminal antennas and emitted power can be respectively smaller and lower, due to signal regeneration on-board the satellite, which was achieved with those on-board routing functions.
In nowadays satellite networks, the link between satellites is not transparent, because it is adapted to a defined protocol type, complicating the construction of satellite payload so the system must be truly reliable, because repairs in outer space are not considered[BWZ00].

2.3 Iridium Satellite System

Despite the existence of four classifications for Geocentric satellite orbits, on this thesis it were only considered the LEO satellite orbits, which have satellites with a minimum altitude of 500 km and maximum altitude of 2000 km[BWZ00]. LEO satellite constellations are promising solutions for satellite networks, for the sake of their low delay and bit error

characteristics [NBSL11].
Among several LEO satellite system, the popular Motorola's Iridium system, was chosen to be the constellation used as reference for this research work. It was completely deployed in May 1998[PRFT99]. The Iridium constellation has 66 cross-linked operational satellites, plus seven in-orbit spares. These 66 satellites are divided in groups of 11 satellites per plan, resulting in 6 planes, each one with eleven satellites. All the satellites belonging to this constellation are located 780 km above the Earth's surface, which means that they are operating at LEO.
Satellites that are part of Iridium system use ISL to route traffic. Call setup procedures and the interface of Iridium with the existing public switching telephone network (PSTN), are handled by regional gateways[PRFT99]. Iridium provides a network where the satellites communicate with other satellites that are near and in adjacent orbits. This kind of operation allows a simple call to roam over several satellites, coming back to the ground when downlinked at an Iridium gateway, and patched into an PSTN for subsequent transmission to destination.
The Existence of 48 spot beams with 402Km of diameter apiece on the Earth's surface for each satellite, is important to decrease the probability of existing dropped calls or missed connections.
Satellites are programmable, so it is possible to upload new instructions to them, in order to maintain good performances and high reliability levels[www10].

2.4 LEO Frequency Range

The most important bands related to this thesis are L-Band (1610 to 1626.5 MHz) and S-band (2483.5 to 2500 MHz), which are typically used by LEO systems for telephone and Short Message Service (SMS).
Ultra High Frequency (UHF) and Very High Frequency (VHF) ranges (137 to 401 MHz) are commonly used by small Low Earth Orbit (LEO) systems to provide low data rate transmissions, so none of them is appropriated for multimedia services. Multimedia transmissions are made in Ku (10 to 18 GHz) and Ka bands (18 to 31 GHz). Ku band is used to provide data communications to the subscriber, and the channel that corresponds to the communication from the subscriber is in Ka band.
A much wider bandwidth for multimedia systems is given by V-band (40 to 75 GHz). The technology that is needed to communicate in this higher range is not much developed, so more research on this subject is needed. It is known that V-band networks will use stratospheric platforms located at an altitude around 20 km to avoid atmospheric precipitation issues [BWZ00].

2.5 Multiple Access Techniques and Channel Achievement

In satellite systems, there are several ways to define separate communication channels, which can be assigned to a single terminal or shared by several [Ret80]. Frequency Division Multiple Access (FDMA), Time Division Multiple Access (TDMA) and Code Division Multiple Access (CDMA) are common access techniques, but other techniques that have been widely deployed in recent networks like Orthogonal Frequency Division Multiplexing (OFDM) and Single Carrier - Frequency Domain Equalization (SC-FDE) will be approached in this section too.

2.5.1 TDMA

By using TDMA, users are able to share the same frequency channel, splitting the signal in different time slots, hence multiple users can share the same transmission medium.
TDMA has some advantages, like easy adaptation to data transmission and voice communication, or the insurance of no interference from simultaneous transmissions, since the users are separated in time.
Disadvantages of using TDMA could appear when a user is moving from one cell to another, and if all time slots in new cell are being utilized, a disconnection might happen. Another problem that can be present in TDMA is multipath distortion. In order to overtake this problem, a time limit can be implemented; if a signal arrives after that time limit, it is ignored. TDMA schemes need to maintain time slots synchronized, so high synchronization overhead is required. The use of TDMA in the uplink brings the requirement for adaptive time advanced required variation, due to terminals and satellites movement.
This multiple access technique is used in Global System for Mobile Communications (GSM) and Satellite communications.

2.5.2 FDMA

FDMA is a multiple access technique where users allocation is made in different spectrum frequencies, allowing simultaneous transmissions (full duplex). Individual channel assignment is made to users on demand. In FDMA, terminal and satellite transmit simultaneously and continuously after the voice channel assignment, avoiding much of the overhead required on TDMA systems [Rap09]. As all users access at the same time but in different frequencies, interference could be a problem when all users are "talking" at the same time.
For large bandwidth, FDMA has some limitations due to equalization complexity. FDMA was improved by two additional approaches: OFDM and SC-FDE. These two techniques will be addressed on two following subsections.

2.5.3 Orthogonal Frequency Division Multiplexing

OFDM is an evolution of Frequency Division Multiplexing (FDM), having as a base the spectral overlapping of sub-carriers, and the transmission of those sub-carriers in parallel occupying each a very narrow bandwidth [PA02]. OFDM can compensate the frequency selective fading by equalizing sub-carriers gain and phase. In OFDM, Inverse Fast Fourier Transform (IFFT) is applied on blocks of M data symbols at the transmitter side to generate the multiple sub-carriers. On the other hand, receiver can extract the sub-carriers by applying a Fast Fourier Transform (FFT) on received blocks. In OFDM systems, sub-carriers are modulated with a conventional modulation scheme [O'R89] before being send with a much lower rate than the original, leading to an efficient struggle against multipath fading[PA02][FABSE02].
There is a cyclic prefix whose goal is to avoid Intersymbol Interference (ISI) with the previous block and make the received block look periodic, simulating a circular convolution, allowing an efficient FFT operation. Cyclic prefix carries the repetition of the last data symbol in a block, being consequently discarded at the receiver.
OFDM signal is constituted by the sum of several slowly modulated sub-carriers, and it results in a high peak-to-average power ratio, no mattering if low level modulation is used on each sub-carrier. In order to maintain the linearity over the range of signal envelope peaks that should be reproduced, the transmitter power amplifier must be reduced in some dBs. This increased power back-off will rise the cost of power amplifier, so this can be a disadvantage. Sensitivity to carrier frequency offset and phase noise is another disadvantage present on OFDM systems. The last drawback that is important to be approached is the data packet granularity, which is a problem related to the fact that data packet size must have at least the same length of an FFT block, affecting spectral efficiency of short packet transmissions [FABSE02].

2.5.4 Single Carrier with Frequency Division Equalizer

SC-FDE is an alternative to OFDM, and it is used on this thesis for uplink proposes.
SC-FDE consists in an utilization of only one carrier, having frequency domain equalization. Single carrier radio modems with frequency domain equalization have several characteristics that are similar to OFDM systems, such as performance, efficiency and low signal processing complexity. Single Carrier modulation uses only one carrier, unlike OFDM that uses several sub-carriers, so the Peak average power ratio (PAPR) for SC-modulated signals is lower. As SC-FDE systems have low PAPR, the power amplifier of an SC transmitter does not need a big linear range to be able to support a given average power, so the power amplifier is less complex on these systems. The main difference of both systems is the placement of an IFFT block operation. In OFDM, the IFFT is made on the transmitter side, with the propose of multiplex data into parallel sub-carriers. In case of SC-FDE systems, IFFT operation occurs on receiver side, allowing the conversion for Frequency Domain Equalization (FDE) signals into time symbols. This main feature

gives good possibilities of both systems coexistence. For instance, in 3rd Generation Partnership Project (3GPP) Long Term Evolution (LTE), SC-FDE is used in transmission, and OFDM in reception, avoiding IFFT operation complexity on transmitter side, improving the terminal battery resources [ZCM12]. Figure 2.1 illustrates OFDM and SC-FDE signal processing, and it shows the different location of IFFT block for both schemes.

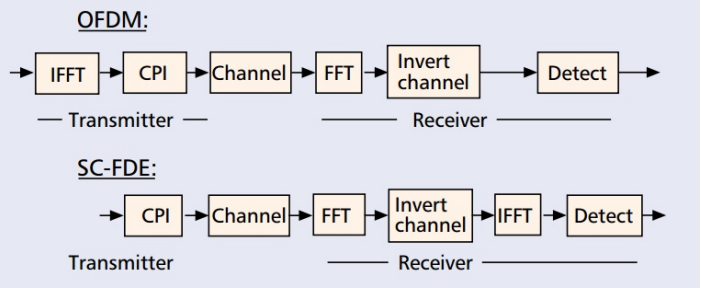

Figure 2.1: OFDM and SC-FDE — signal processing [FABSE02]

2.5.5 CDMA

CDMA multiple access technique allows each station, or in this case each terminal, to transmit over the entire frequency spectrum. Transmissions are distinguished by using a different code each, which is approximately orthogonal. That code allows CDMA on receiver side to despise everything except the desired signal, using a time correlation operation. The receiver has the obligation to know the codeword that the transmitter used, in order to detect the message signal. There is no knowledge among users, so it means that each users operates in a independent way [Tan02][Rap09].
CDMA has a lower capacity limit than TDMA and FDMA, due to the near-far problem. This problem usually happens when a large number of mobile users access the same channel. This problem consists in a strong signal reception from some users, that raise the noise level at the base station or satellite demodulators for weaker signals, so these weaker signals have low probabilities of being received. To avoid this problem, it is possible to implement a power control operation on the satellite. This power control operation involves a sampling of Radio Signal Strength Indicator (RSSI) levels of each terminal, at the satellite followed by sending power change commands back to the overpowering terminals to fix the problem. Power control is used for users inside the same cell; out-of-cell terminals can also cause interference, but this problem is not solvable by the receiver.
As it was said before, the signal is spread over a large spectrum, so this is an advantage, since multipath fading is substantially reduced[Rap09].

2.6 ARQ schemes

Automatic Repeat Request (ARQ) protocols are reliable data transfer protocols that are based in retransmissions. Normally, in this type of protocols, the receiver can inform the

sender of what has been received with and without errors, in order for the sender to retransmit what it was not received correctly. This information exchange is performed by control messages.

ARQ protocols must have three capabilities: error detection, receiver feedback and retransmission. Regarding error detection, it must be known at the receiver by applying error detection techniques. Therefore, the sender must send additional bits beyond the original data to allow error detection. In terms of receiver feedback, it is necessary that the sender knows how the receiver received the information; so messages like Acknowledgement (ACK) or Negative Acknowledgement (NACK) are sent back to the sender. Retransmission refers to the packets that are sent to the receiver again, after being received with errors in the previous transmission[KR09]. There are some transmission control schemes that were created to prevent the sender to flood the receiver with packets at a speed that is faster than the latter can process [Tan02]. Stop-and-Wait algorithm is the simplest ARQ scheme, and it consists in the sender waiting for an acknowledgement before transmitting a new frame. The sender's waiting time is not eternal, because if the ACK message does not arrive a time out happens and the retransmission of the original frame is proceeded [Pet07]. Stop-and-wait could decrease the performance by increasing the delay. A technique that is used to counter this problem is named pipelining, where the sender can send several packets and does not have to wait for acknowledgements. In this case, the range of sequence numbers must be larger, due to the fact that sequence numbers must be unique, and the number of transmitted packets is bigger. There are two schemes that use this pipelining technique: Go-Back-N and selective repeat. Go-Back-N, consists in a sender transmitting a maximum pre-stipulated number of multiple available packets without having to wait for acknowledgements. This maximum number is also known as the window size. In this protocol, the window slides through the sequence number space, so this protocol is also known as sliding window protocol. When the sender receives a NACK from the receiver or after an acknowledgement times out, it transmits again from the first packet that was not acknowledged. A problem is the possibility of several unnecessary packet transmissions, for the packets previously transmitted with success. This problem is more severe when window size and bandwidth delay product are large, leading to large number of packets in the pipeline. In order to avoid this problem, Selective Repeat (SR) protocol was created. In SR, the sender only retransmits the packets that he suspects were lost or corrupted during the transmission. When the sender receives a NACK packet, it retransmits the missing packet. The difference to Go-Back-N (GBN) protocol is that after the retransmission, the sender still transmits the packets that are next in sequence order, and not those that comes next to the one who failed [KR09][Tan02].

2.7 Forward Error Correction schemes

The use of error-correcting codes could also be referred as Forward Error Correction. A strategy used in Forward Error Correction (FEC) is to include redundant information on sent data blocks, allowing the receiver to analyse it and see if data was correctly received, and if not, to know what was the error. FEC differs from error-detecting codes, since they include less redundancy than FEC, only enough for the receiver to know that an error exists, but without knowing what the error is [Tan02]. Forward error correction coding is normally proposed for end-to-end recovery of several packet losses, using redundant packets [KRT11]. These error control systems are usually applied on channels where the information flows in only one direction; in other words, data traffic has a one-way nature. Those type of channels are also known as simplex channels.
The FEC concept arrived during the 1940s by the hand of R.W. Hamming, which invented the famous Hamming codes at Bell laboratories, in order to prevent read errors in punch cards for relay-based electro-mechanical computers. From 1950s to 1970s new codes were born and consequently algorithms were created to handle those codes. Cyclic codes were established like Bose–Chaudhuri–Hocquenghem(BCH) codes, Reed–Solomon (RS) codes, Reed–Muller codes, that have as decoding algorithms Berlekamp–Massey algorithm , and Euclid algorithm. Convolutional codes were also developed, decoded with the Viterbi algorithm [Miz06].
During the evolution of FEC codes three generations can be identified. The first generation of FEC codes used linear block codes; it is based on hard decision decoding, which is a single quantization level in a bit sampling. Concatenated codes, as the name suggests, is a junction of more than one type of code. The utilization of concatenation codes along interleaving and iterative decoding allows a better performance of errors correction. These concatenation codes are known as the second generation of FEC [Miz09] [Miz06]. Despite the second generation has better results than first in terms of coding gain, it has a problem of compatibility, because second generation FEC frame structures are not compatible with all systems. Turbo codes and Low Density Parity Check (LDPC) codes were created in an attempt to surpass this issue and to increase the power of FEC representing both the newest generation of FEC, which is the third generation, based on soft decision and iterative decoding. Nowadays, turbo codes are often used in communication systems[FC07], in view of being the most powerful codes, almost achieving Shannon's theoretical limit. This limit was discovered by Claude Shannon in 1948, and says what is the maximum data rate, taking into account the physical channel capacity[Sha48]. Turbo codes consists in a parallel concatenation of more than one code, and they are associated with soft inputs and soft outputs decoding. There are two types of Turbo Codes (TC): Convolutional TC and Block TC. The first type uses a parallel concatenation of convolutional codes, the second one uses a block product code. The latter is better for transmissions that require low redundancy [ASL00].

2.8 Hybrid ARQ Schemes

Hybrid-ARQ schemes are known as the combination of ARQ and FEC schemes, both approached in previous sections. When this combination is done in a proper way, the disadvantages of both schemes can be overcome [LCM84].
In order to classify an ARQ protocol efficiency, it is necessary to measure the throughput, which is the "average number of user data bits accepted at the receiving end in the time required for transmission of a single bit" as it is defined in [GKVW04]. Therefore there is a trade-off between successful transmissions and quantity of user data in the frame, due to redundancy level of FEC in Hybrid-Automatic Repeat Request (H-ARQ) schemes. In order to find a balance for both effects it selected a fixed rate code that is appropriated to channel characteristics and throughput requirements[GKVW04].
The option of including FEC schemes in ARQ protocols was taken because it allows a correction of frequent error patterns, decreasing the number of retransmissions and increasing the system throughput. Another advantage and drawback surpass, is related to the H-ARQ ability of allowing the receiver to request a retransmission even when a uncommon error pattern is detected. H-ARQ has higher reliability and throughput than standalone FEC and ARQ schemes respectively.
The H-ARQ schemes can be divided in two categories: Type-I Hybrid ARQ and Type-II Hybrid ARQ [LC83] [LCM84], which are approached on following sub-sections.

2.8.1 Type I Hybrid-ARQ

The type I of hybrid ARQ protocol is the simplest of hybrid protocols, and it uses one-code or two-code systems. On this protocol, each packet is encoded for error correction and error detection error control systems [Wic94] . The message and the error detecting parity bit are encoded using an FEC code. The error correction parity bits are used in order to correct channel errors at the receiver side. A message estimation and the error detection parity bits are outputted to an FEC decoder, which tests it for error detection to determine if the message should be accepted or rejected due to errors.
When the message is long or the channel signal strength is low, Type I H-ARQ can increase the efficiency, because this protocol decreases unsuccessful transmissions probability by adding extra FEC parity bits. It is possible to have a coding gain if a compensation between the reduction of transmissions and the increase of message length is made.
There is a crossover point in terms of strength between ARQ protocols and Type I H-ARQ protocols when the protocol's efficiency is the main subject. It happens in cases where signal strength is high. In this cases, this hybrid protocol type does not improve the efficiency, because the strong signal allows a deliver of free error messages. So the extra FEC parity bits are wasted, hence this H-ARQ protocol type is not the best option in this case, as opposed to plain ARQ protocols [CC84].

2.8.2 Type II Hybrid-ARQ

Type II H-ARQ protocol is mainly based in incremental redundancy, because it permits the protocol to adapt to changing channel conditions. Additional parity bits are send by the transmitter in response to retransmission requests that were sent by the receiver. The increased correction capability is allowed when the receiver appends those parity bits to the received packet [Wic94].
In [CC84] it was stated that this type of scheme does not send FEC parity bits with message and error detecting parity bits. There is an intercalation between message bits with detecting parity bits and FEC parity bits on transmissions. When the message is received without errors, the FEC parity bits are not sent. The main goal of Type II H-ARQ protocols is to work with the efficiency given by plain ARQ protocols in strong signals and to obtain the improvement of type I H-ARQ when the quality of the signal is low.

2.9 Multiple-Input Multiple-Output (MIMO) systems

Multiple-Input Multiple-Output (MIMO) communications exploits the physical channel that is between multiple receiver and transmitter antennas. MIMO systems provide an spectral efficiency increase for a given power transmission. The introduction of additional spatial channels, that are exploited by space-time codes, increase the network capacity. It increases linearly with Signal-to-noise ratio (SNR) for low SNR and logarithmically with SNR for high SNR. The channel estimation information in MIMO systems can be fed back to the transmitter, enabling it to adapt. Although the systems without feedback can be simpler to implement, with high SNR, the spectral-efficiency bound is similar to an informed transmitter.
To implement a MIMO communication system it is necessary to implement a particular coding scheme. Space-time codes provide the exploitation of MIMO degrees of freedom, enabling spatial and temporal redundancy in the data received by an array of antennas, and spectral-efficiency increase. Space-time coding can have two basic approaches. In the first one, the receiver informs the transmitter about the propagation channel information, so the transmitter can adjust its coding. This approach has advantages in terms of capacity, but it can be difficult to apply in dynamic environments. The second approach implements fixed codes of several rates, offering good performance over all channels. These fixed codes share transmitted power equally among all spatial channels [BFC05].
MIMO systems brings several advantages over single-antenna-to-single-antenna communication, which is also known as Single-Input Single-Output (SISO). MIMO systems have less sensitivity to fading due to the existence of multiple spatial paths, which is known as spatial diversity. Reduction of power is another advantage over the SISO systems, and a study in [BFC05] revealed that a lower energy per information bit $\frac{E_b}{N0}$ is needed, for higher number of antennas on receiver and transmitter side. Figure 2.2 illustrates it, by showing that a higher number of antennas on both sides (receiver and

transmitter), obtains a greater spectral efficiency with less energy per information bit.

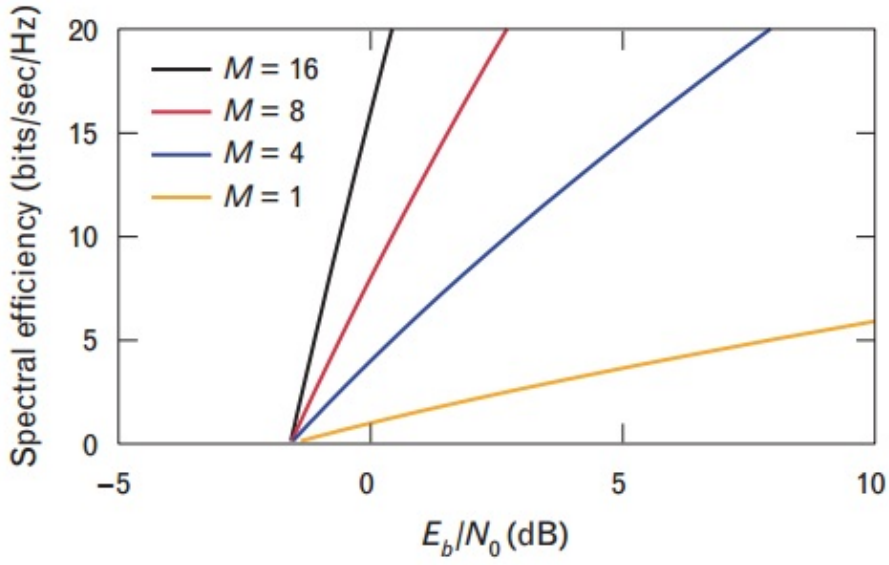

Figure 2.2: Spectral-efficiency bound as a function of noise-spectral-density-normalized energy per information bit $\frac{E_b}{N0}$ [BFC05]

2.10 MAC Protocols in satellite communications

The main goal of Medium Access Control (MAC) protocols is to control the access of communicating stations to the wireless medium, to share the network bandwidth.
Not all MAC protocols are useful to satellite communications, because some requirements are not achieved, primarily due to the long propagation delay. A large range of protocols that are applied in LANs and WANs can not be used for this purpose. "Fundamental architectural objectives in the design of MAC protocols for satellite communications are high channel throughput, low transmission delay, channel stability, protocol scalability, channel reconfigurability, and low complexity of the control algorithm" [Pey99].
In satellite communications, MAC protocols should also enable quick fixes to networks failures and easy solutions to topology changes. The goal of these MAC protocols is to satisfy QoS requirements, achievable applying Demand Assigned Multiple Access (DAMA) or an hybrid mode with random access and reservation mechanisms. The next three sub-sections address these MAC protocols with demand assignment, random access, reservation and an hybrid protocol that is a mixture of random access protocols and reservations protocols [Pey99].

2.10.1 Random Access Protocols

Random Access Protocols are contention oriented protocols. The main difference compared to contention-free protocols is that in contention oriented protocols transmissions, stations do not have guaranteed success in advance [Pey99].
Contention protocols have a maximum throughput percentage stipulated, which depends on the protocol simplicity. Results vary from 18 percent for simplest protocol (Aloha) to 50 percent on sophisticated ones. The most common protocols, use a form of Slotted Aloha, and reach maximum throughput values around 36 percent [Fel96].
Random access protocols can be very advantageous regarding implementation, because they are simpler, and adapt to varying demand. Random access, can also be disadvantageous, due to the fact that collisions may happen, so it can lead to a wasteful of capacity. This problem can result in lack of real-time application accommodation and non-guaranteed Quality of Service (QoS).
Satellite communications have a long Round-Trip-Time (RTT), so packet collisions can aggravate propagation delay, since each packet collision adds in the best case, one round-trip delay to the packet transmission time [Pey99].
An example of networks that apply random access protocols are Very-small-aperture terminal (VSAT) networks, which consist in transmissions of data bursts by small earth stations.
Pure Aloha, Slotted Aloha or Carrier Sense Multiple Access (CSMA) are examples of protocols that use random access. In Pure Aloha, stations are not synchronized, and only transmit packets when they are ready. When a collision occurs, each user knows that it happens and retransmits the packet after a random period. This random period provides stability to the protocol. In CSMA, each station senses the channel before accessing it to verify if any transmission is occurring. When a transmission is successfully completed, each ready station transmits with a probability 1 into the next time slot; if a collision occurs, an adaptive algorithm is executed by every station, calculating the probability in the next time slot. CSMA does not detect collisions, but there is a derived protocol named Carrier Sense Multiple Access with Collision Detection (CSMA/CD), where stations abort transmissions after detecting collisions [Pey99].

2.10.2 Demand Assigned Multiple Access

DAMA is a class of multiple-access techniques, hence terminals or users are able to share available satellite resources [Fel96].
DAMA protocols can allocate capacity based in FDMA or TDMA architectures. DAMA protocols are suitable to situations where the traffic pattern is random and with large variations, in view of the protocol ability to allocate capacity on demand, avoiding inefficient use of transponder capacity [Abr92]. MAC protocols that apply DAMA can use bandwidth efficiently and increase the throughput, due to the ability to allocate capacity

on demand, following the station capacity requests. This reservation on demand, as reported earlier, could be explicit or implicit [Ret80]
Regarding implicit reservation, stations compete for reservation slots by using Slotted Aloha. Slotted Aloha is a way to allocate users, by taking into account consensus among users on slot boundaries definition. Slot synchronization can be obtained by having a satellite working like a clock, which is by emitting a pip at the start of each interval [Tan02]. By using slotted-Aloha protocol, the satellite channel is slotted into segments with a duration exactly equal to single packet transmission time. Slotted-Aloha eliminates the partial overlapping, because terminals are synchronized to start the transmission of packets at the beginning of a slot [Ret80].
In Explicit Reservation, all frames have a control subframe with a sequence of bits, that serve to announce or reserve upcoming transmissions. In these frames, a single reservation slot is assigned to each station or terminal . This type of reservation scheme reserves future channel time, in order to send messages to a specific station.

2.10.3 Reservation Protocols

The main goal of reservation protocols is to avoid collisions. Therefore the users distribution leads to the need of a reservation sub-channel, in order to give ability for users to communicate with each other, since only one station can access the channel at a time.
A large number of reservation protocols use the TDMA protocol or some kind of slotted-Aloha protocol. As it was said before, TDMA could be inefficient for bursty traffic that comes from several users. On the other hand, the number of users is irrelevant for S-Aloha protocol, but user access has to be adaptively controlled for stable operation [Pey99].
In this type of protocols, it is possible to gain in terms of channel stability, by cutting channel control mechanism, and vice-versa. By using contention oriented protocols, channel throughput can be increased, but as a consequence, message delay is going to increase too. Excluding message transmission time, the minimum delay caused to a message is more than twice the channel propagation time [Pey99].
Some types of reservations protocols are Reservation Aloha, Priority-Oriented Demand Assignment and Assigned Slot Listen Before Transmission [Pey99].

2.10.4 Hybrid of Random Access and Reservation Protocols

A MAC protocol using an hybrid mode of random access and reservation protocols is considered on this research work, where the best characteristics of random access and TDMA are present. The terminals compete among them during the reservation period. This dispute has some winners, which are the ones who had success in making reservations, hence these users transmit without contention during the transmission period.
A main characteristic of hybrid protocols is that their reservation period is much shorter than transmission period, so this is where their efficiency derives [Pey99]. A known

Hybrid-Medium Access Control (H-MAC) protocol is Aloha Reservation (Aloha-R) protocol. In Aloha-R protocol, the frame is divided in slots and the slots are divided in mini-slots. Slotted-Aloha is used to obtain the mini-slots and they are seen as a common queue to all users. Reservation is made for data slots, and its number depends on current load. When a station wants to transmit, it uses a mini-slot to send a packet requesting a number of mini-slots to transmit data. When this reservation is successfully done, the station knows what slots it has acquire. A First-In First-Out (FIFO) process is used to determine the order of reserved slots for each station; in other words, the first to request the slots to transmit, is the first to obtain them [Pey99].

2.11 Physical Layer solutions

This layer has the function of converting data into bits and vice-versa, depending if it is for transmission or reception proposes respectively. In the transmission process, the physical layer receives data from upper layers and converts it to bits. The reception process is the inverse, with the physical layer receiving the bits that were sent from another node, and converting them into data, that is gathered into frames and passed to upper layers. The medium compatibility is important in connections among devices, so this layer has an important role by encoding the frame in a certain format, allowing the communication between the nodes. Another PHY-Layer main functions are the signal generation and the timing and synchronization among devices [BNNK08].
In [ZR94][HKL97] was observed, that the signal capture mechanisms can decode a packet that has a higher power, in comparison with all the other packets involved in a certain collision. This means that PHY-Layer can be used to solve packet collisions problems, which leads to a conclusion that nowadays these problems could not be exclusively solved by MAC layer. The next sub-section provides a explanation of Multiple packet reception systems, which is a PHY-Layer solution to issues involving packet collisions.

2.11.1 Multiple Packet Reception

Research work is being done to suppress the loss of throughput, produced by increasing the number of users communicating in wireless networks. Multiple Packet Reception (MPR) can be defined as the ability of receiving and decoding more than one packet from concurrent transmitters; in other words, it is the capability of receiving packets that are involved in collisions [LSW12]. This MPR characteristic in PHY-layer makes the packet transmission less restrained than it is on conventional medium access protocols, where only one packet is received at a given time. Hence, it may leads to an increase in system throughput. In order to improve networks throughput, new MAC protocols have to be designed more adapted with this PHY-Layer characteristic. Multiple Packet Reception is currently an active area of research [ZZL06, RP12].
MPR is normally realized with CDMA or MIMO techniques, where the first one is used

on the transmitter perspective and the latter in the trans-receiver perspective, where transmitter and receiver cooperate on some operations. CDMA on transmitter side, allows the receiver to decode multiple data streams by knowing the different codes. In order to enable Multiple Packet Reception, cooperation between transmitters and receivers is required in some operations. A MIMO system has multiple antennas on both sides (transmitter and receiver), and each antenna has different channel characteristics; therefore packets that are sent from different antennas can be distinguished using channel estimators [LSW12].
The signal separation is an issue associated to MIMO system, so [vdVT02] developed an algorithm named Known Modulus Algorithms (KMA), in order to allow packet separation in asynchronous ad-hoc networks. This algorithm consists in a constant modulus signal that is sent by the transmitter multiplied by an amplitude modulated code, which is known at the receiver. The receiver has also an array of antennas that allows the detection and consequent filtration to obtain the desired user, despise the other ones.
A technique to provide MPR capability was developed in [OLLMML03], where the authors used the baseband signal cyclostationary properties, that appear after a modulation with specific polynomial phase sequences. Therefore a bandwidth expansion is not made by proposed modulation, which can be considered as a *colorcode* to distinguish different users packets.
There are techniques that do not need a cooperation between transmitter and receiver functions to have MPR, because only the receiver is able to decode several packets at the same time. Multi-User Detection (MUD) schemes that stands on the receiver side are appropriated for MPR. In [WSGLA08, WGLA09] the authors used these techniques to create MPR, alleviating the interference created by multiple transmissions.
Sub-optimal MUD techniques can be linear or non-linear. Decorrelated detectors [LV90] and Minimum Mean Square Error (MMSE) detectors are the most known linear MUD techniques, which have an advantage of yielding an optimal value for the near-far resistance performance metric, but these linear techniques have also as drawback its high complexity. This disadvantage is not present on non-linear MUD schemes, because the complexity is much lower, but the performance of these schemes is worst. Non-linear MUDs have the main function of removing interference from the received signal. The most known in this category is the Multistage Interference Cancellation (IC) that can have two forms of interference cancellation: Successively Interference Cancellation (SIC) [WSGLA08, WGLA09] and in Parallel Interference Cancellation (PIC) ways [BCW96].

2.12 PHY-MAC Cross-layered Designs

As the name of the section indicates, two layers of Open Systems Interconnection (OSI) model are involved on the cross-layer architectures presented in this section: Physical Layer and MAC Layer. The OSI reference model usually specifies that layers do not

share information between them. In a Cross-Layer Design for Wireless Networks it is assumed that it is important to share information on lower layers in order to improve the performance on higher layers in terms of wireless communications.
The Cross-Layer concept refers to an interaction between protocols that are at different layers of the OSI protocol stack. This interaction brings some advantages, because all levels of network protocol stack are affected by wireless link characteristics, hence all layers must respond to changing channel conditions, leading to a strong union among protocols at different layers. Some conditions have to be present at all layers in order to provide QoS delivery and adaptability to channel transmission. For instance, at the physical layer, dynamic adjustment of receiver filters can be made to respond to interference changes; at the link layer, the interference level can be affected by adapting power, rate and coding; finally at the MAC layer, it is possible to adapt scheduling, based on the current level of interference and on the quality of the current link [BNNK08]. Over the years some research work has been made to develop cross-layered protocols. The authors of [CLZ08] created a MAC-PHY algorithm for ad-hoc networks that utilizes Vertical-Bell Laboratories Layered Space-Time (V-BLAST), which is an architecture that provide very high data rates over a wireless channel [WFGV98]. A union of MPR with MAC and a creation of an adaptive resource allocation algorithm for MIMO Wireless Local Area Network (WLAN) was made by [HLZ08]. In [GLASW07] a study of a cross-layer MAC algorithm for WLAN having single antennas terminals and multiple antenna access points was made taking into consideration an error free transmission channel. In [RP12] it was studied a Cross Layered MAC-PHY algorithm with MIMO and over a jittery channel, revealing a high SNR and a low bit error rate.
As a result of several research works, a scheme having PHY-MAC resolutions gained some relevance; its name is Network-assisted Diversity Multiple Access (NDMA), which is approached in the next sub-section.

2.12.1 Network Diversity Multiple Access

NDMA was created by Tsatsanis [TZB98] in order to avoid unnecessarily discarding of colliding packets, for the reason that the signals with those packets can have some mixtures of useful user packets information. The study in [TZB98] consisted in doing a selective retransmission of corrupted packets, using the network to create diversity. Separation techniques are used to recover the user packets. This scheme has the main goal of transmitting the packets from q collided users by using q slots (packet transmissions), preserving the channel throughput with collisions.
The received signal from collided packets are stored in memory, and it is combined with future retransmissions, allowing the extraction of collided packets', information.
When a collision occurs, this technique guarantees that none of the packets slots are lost, having this as its biggest advantage. As it was referred earlier, throughput is not penalized, because the number of collided users is equal to the number of required slots, and

is also equal to the number of transmissions information packet. This technique does not affect the PHY-layer bit rate parameters of each source for the reason that it is mostly indicated for multiplexing variable-bit-rate sources, due to the fact that if some users experience big amounts of load or unstable queues, the performance gets worst, being compared to a q-TDMA system.
After *Tsatsanis et al.* published this technique, some research work was done in order to evolve it. The initial NDMA was designed for flat fading channels, which are not very appropriated for wireless communications. So in [ZT02] it was built a new strategy for a frequency selective channel environment using multiuser receivers and CDMA systems. They implement transceiver architectures and random access strategies to separate collided packets when unknown propagation channels are present. ID signature sequences were used, making easier the collision detection and resolution process when multipath effects are present. This work revealed a maintenance of good throughput performance. A disadvantage that is brought by ID sequences is that they grow linearly instead of logarithmically with the number of users, introducing a considerable overhead process. By taking this issue into account, in [ZST02] methods were developed to resolve packet collision problem without the need of an orthogonal ID sequence; those methods are known as blind signal separation methods. The blind method differs from the original NDMA by being less computationally demanding due to its proportionality to the number of colliding packets, unlike [TZB98] method which whose proportionality was relative to total number of users in the system.
A new evolution of NDMA scheme that was used on this thesis was Hybrid-NDMA scheme, which will be approached in following chapter.

2.12.2 Hybrid NDMA

The combination of an H-ARQ technique with NDMA was proposed by *Ganhao et al.* in [GPB+11], who named this mechanism by Hybrid-ARQ NDMA (H-NDMA). Basically, the access mechanism forces (Mobile Terminals) MTs to transmit a quantity of packets copies greater than the number of collided MTs. The Base Station (BS) defines the time slots, which are used by MTs to send data frames. Several MTs could use a given channel, and the maximum number Z that is doing it, is controlled by the BS. The Base Station has also the duty of detecting collisions and to inform the MTs that it occurs through a broadcast downlink channel. After the involved MTs received the collision information signal, they resend their packets.
H-NDMA is considered by *Ganhao et al.* a "slotted random access protocol with gated access", allocating the uplink slots in a organized way, which can be called by a sequence of epochs, and using an SC-FDE scheme for uplink proposes. The BS transmits a synchronization signal (SYNC) to alert the MTs that a epoch is starting, so they are allowed to transmit at the next slot. MTs with new packets to transmit wait for the start of a new epoch. Each epoch is defined by the number P of MTs that transmit data, and it was

assumed that this number fits $1 \leq P \leq Z$. When P MTs are linked to a collision, the base station requests P-1 retransmissions. An ACK signal is sent by the BS to MTs, defining the ones that must retransmit at the next slot. This stipulated epoch ends when all packets are correctly received, or when the maximum number of additional retransmissions are send.
This research work concludes that H-NDMA has advantages in terms of network capacity and packet delay when compared with the classics NDMA MAC protocol and Hybrid-ARQ protocol. Scalability was another characteristic shown by this new protocol. The performance gets better when more MTs transmit in a certain epoch.

2.13 Handover in Satellite Systems

As this thesis focuses in LEO satellite systems, it is important to refer that satellite speed on Iridium constellations is extremely high (27000 km/h), and because of that, handover process happens frequently. There are two types of handover in LEO satellites constellations, which are classified in link-layer and network-layer handover [CAI06a]. Before starting a more specific explanation about these two handover types, it is important to emphasize two things: The first is to mention the two different schemes that were created to approach cellular coverage geometry for LEO satellites: Satellite Fixed Cell (SFC) systems, which are the ones focused on this research work, and Earth Fixed Cell (EFC) systems. In SFC systems, the cell position relative to satellite does not change, i.e, the cells on the ground move synchronously with the satellite. In EFC systems, the earth's surface is divided in predetermined cells with fixed boundaries; so the satellite has a stipulated time to be assigned with a fixed cell [Ngu02].
From the user standpoint, it is preferable to block a new arriving call than to interrupt a conversation. One way to handle this issue is by allocating resources before starting any handover operation, in order to reduce the probability of a forced termination. Another approach is by queuing handover (QH) requests, which are placed for a maximum time interval, which is equal to the time period of MTs existence in a area that is covered by two satellites. This handover request queueing is made in case of lack of channel availability in the destination cell [MAEIB12].
When a change of user's Internet Protocol (IP) address occurs due to the change of satellite's coverage area, a network-layer handover is going to proceed, transferring the current connections of higher-level protocols to a new IP address [CAI06a]. Network-layer handover schemes can be of three types: hard handover, soft handover and signalling diversity (inter-segment) handover. In hard handover, the current link is released, and only after this happens the next link is established, allowing a new connection to a different satellite. In soft-handover, the terminal user only turns off the first link when a second link is connected, which means that before the handover process is complete, the user has two links, each connected to different satellites, but the data only flows through the new link. Finally, in Signaling-diversity schemes, data packets flows through both links, the

old and the new, generalizing the soft-handover schemes. Regarding the link-layer handover, QoS is taken into consideration to evaluate the handover performance. It is done by considering the probability of having a blocked call, and the probability of a call being dropped, both during handover process, existing a trade-off between them. This type of handover occurs when one or several links between communication endpoints need to change, due to the dynamic connectivity pattern in LEO systems. Link-layer handover can have three categories: spot-beam handover schemes, satellite handover schemes and ISL handover schemes [CAI06a].

2.13.1 Spot-beam Handover Schemes

The spot-beam handover occurs inside one satellite coverage area, which means that other satellites are not involved in this process, so it is also called intra-satellite handover. This handover occurs when the terminal crosses the boundary between spot-beams that are under a unique satellite coverage. Actually it is not really the terminal that moves across the spot-beams, but the satellite movement related to Earth provoke a constant movement of spot-beams, so they are constantly passing over a fixed point on Earth's surface. As the spot-beam areas are small, intra-satellite handover are frequent [CAI06a, NLSvA01].

2.13.2 Satellite Handover Schemes

The name of this scheme is actually very self-explanatory, for the reason that the handover is between different satellites, i.e., the user's attachment point is transferred to another satellite. In [NLSvA01] was presented a study of handover on satellite IP networks, and proposed two types of satellite handover: proactive handover and reactive handover. The first one is based on handover prediction, so the current satellite asks the new satellite for resource reservations before starting the handover process. In the latter case, there is not any kind of preparation, which means that resources reservation is done only when the user asks for an handover. Proactive handover schemes are more complex comparative to Reactive handover schemes, because the first one needs more network resources and computation overhead. However, in LEO constellations, the satellites positions are easily known and handover can be predicted in advance, so proactive handover is more appropriated for them. An illustration of satellite handover is present in figure 2.3.

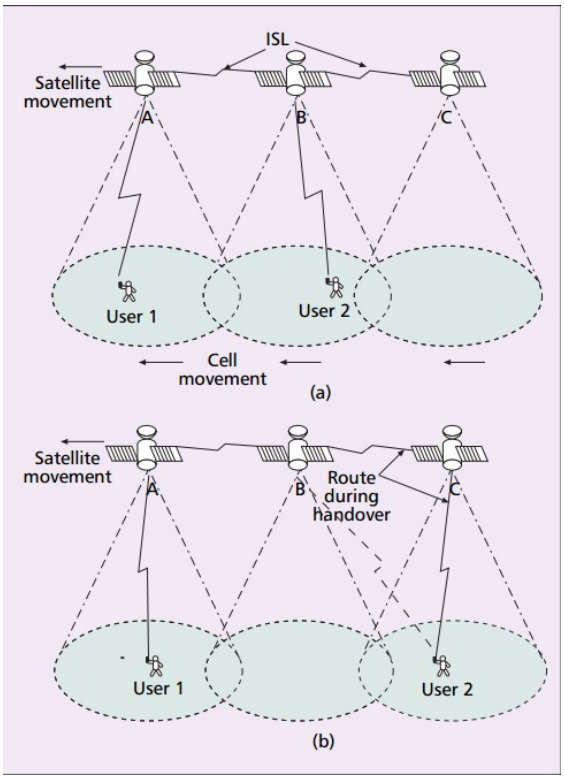

Figure 2.3: Satellite handover: a) initially, user 1 and user 2 communicate through satellite A and B; and b) after user 2 hands over to satellite C, the communication is through satellites A, B, and C. Figure from [CAI06a].

2.13.3 ISL Handover Schemes

ISL handovers happens when LEO satellites are in polar areas. In neighbouring satellites, changes of connectivity patterns occurs, i.e, changes in distance and viewing angle between satellites that are neighbours are the reason why ISL are temporarily switched off. When this occurs, ISL are rerouted producing ISL handovers [CAI06b, CAI06a].

3

Satellite Communications

This chapter covers the first part of this research work, which consists in a study in terms of throughput, packet transmission delay, and energy consumption, by taking into account a vertical line (no angle) communication with a LEO satellite. It was considered a fixed distance of 780 km between the terminal and satellite. QoS constraints are considered, in order to allow voice communication services.
This chapter describes minutely the proposed schemes and the protocols that were used along the physical parameters. Some illustrations and descriptions of how the communication with one satellite was idealized are presented in this chapter too.
As the communication between MTs and satellites involves large distances, Round-Trip-Time (RTT) is too large, so an H-NDMA scheme is not efficient to handle this problem, since it was designed for shorter distances [GPB+11]. A S-NDMA protocol is proposed as a solution to overlap this issue. This chapter presents the design of S-NDMA and a comparison based on simulation results with H-NDMA protocol.

3.1 System Characterization

The uplink transmission in a satellite system is considered in this thesis. A set of MTs send data to a satellite. MTs are low resource battery operated devices, whereas the satellite is a high resource device that runs a multi-packet detection algorithm with H-ARQ error control in real-time. The MTs send data packets using the time slots defined by the satellite (for the sake of simplicity, it is assumed that the packets associated to each user have the same duration). This thesis considers a pure DAMA approach: before transmitting in the uplink channel, a MT sends a transmission request through an uplink control channel. Besides defining time slots, the schedule specifies which MTs transmits in each

slot (there can be more than one per slot) and what transmission power is used. The uplink scheduling is selected using the optimization algorithm proposed in the following sections.

3.2 Medium Access Control Protocol

In S-NDMA, the slots in an uplink data channel, from the MTs to the satellite, are organized as a sequence of super-frames, where the MTs' transmissions are scheduled after a request. Packets are transmitted within epochs, that may involve several MTs and be distributed over up to $R+1$ super-frames. Individual packets are firstly scheduled to $P+n_0$ slots in an initial super-frame for P transmitting MTs, where $n_0 \geq 0$ defines a number of redundant retransmissions used to improve error resilience. It is assumed that the satellite is capable of discerning all colliding data packets using user-specific orthogonal ID sequences defined in the schedule. The initial number of packets' transmissions allows the separation of all P packets transmitted simultaneously [TZB00]. However, due to channel errors, some of the packets may not be successfully received, so additional slots may be scheduled in future super-frames. An epoch ends when all packets have been correctly received or after the $R+1$th super-frame. Besides the scheduling information, the downlink control channel supports the exchange of acknowledgement information about the packets received in each slot. The number of packet transmissions in the sth super-frame is denoted as n_s, where $s \leq R$, and the vector with all n_s values is denoted as $\mathbf{n} = [n_0, n_1, ..., n_R]$. The time interval between two successive super-frames of an epoch (used to transmit a given packet), T, is at least above the longest RTT measured by the furthest MT. Therefore, R will be bounded by the delay requirements specified for the QoS traffic class that is being transmitted on a given epoch. It should be noted that H-NDMA defined in [GPB+11] is a special case of S-NDMA, where $\mathbf{n} = [0, 1, 1, ..., 1]$. This means that S-NDMA trades off a lower delay for a higher energy consumption per packet transmitted. Figure 3.1 illustrates an epoch in the S-NDMA slotted access scheme, where $P = 2$ MTs are scheduled for $R = 2$ and $\mathbf{n} = [n_0, n_1, n_2]$. MTs A and B transmit the packets in $2 + n_0$ slots of the first super-frame and in n_1 slots of the second. MT B does not transmit in the third super-frame of the epoch, since its packet was successfully received after the second super-frame. Information regarding which packets are received in a given epoch, can be passed to physical level by a matrix present in figure 3.2. This matrix contains information of $P = 4$ users and a total number of slots allocated to an epoch $\zeta_l = 4$, in a case where three terminals transmit on the first epoch, one terminal transmit at the second, and none at the third epoch. In Figure 3.2, it is presented a case where $n = [2, 1, 1]$, so in the first super-frame of the epoch $P + n_0 = 6$ copies of packets are transmitted, on the second super-frame of the epoch $n_1 = 1$ copies, and on the third super-frame of the epoch $n_2 = 1$ copies. This information can be used to calculate the Packet Error Rate (PER), considering the error of collision probabilities due to scheduling composition.

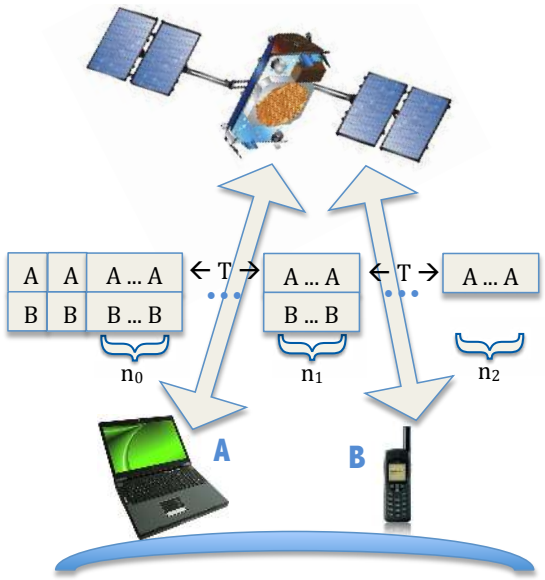

Figure 3.1: S-NDMA Demand Assigned scheme

J	J	J	J	n0	n0	n1	n2
1	1	1	1	1	1	0	0
1	1	1	1	1	1	0	0
1	1	1	1	1	1	0	0
1	1	1	1	1	1	1	0

Figure 3.2: Mapping to physical layer matrix example

3.2.1 Handling very low power using CDMA

The high distance between satellites and MTs and the limited transmission power in the MTs introduce a challenge in the design of S-NDMA with a large number (hundreds) of retransmissions that allow the correct reception of the transmitted packets. This is not possible in a physical implementation due to the complexity of the H-NDMA receiver algorithm.
This thesis proposes a solution to reduce the H-NDMA receiver complexity. The solution combines H-NDMA and CDMA, and group slots into CDMA frames applying the H-NDMA receiver algorithm to the CDMA frames. This decreases the number of packets handled by NDMA by a spreading factor S_f. Besides the lower NDMA complexity, the noise power is also reduced, due to the channel spreading factor gain. When the narrow band signal is transformed into a CDMA signal by a spread spectrum operation, the original channel bandwidth is replaced by a channel bandwidth S_f times higher. Since the original bandwidth is now replaced by the bandwidth of the CDMA signal, the spectral efficiency of the system is reduced by S_f times. Therefore, the S_f value must be chosen to assure the best trade-off between NDMA complexity and transmission data rate. It should be mentioned that a higher value of S_f decreases NDMA's complexity and transmission data rate and a lower S_f value does the opposite. A value of $S_f = 128$ was chosen for a LEO scenario, by taking into account the mentioned trade-off balance. This number allows the reception of packet with less than ten CDMA frames.

3.2.2 Multipacket Detection Receiver Structure

This thesis considers the uplink transmission of a satellite system with SC-FDE. We adopted the uncoded multipacket detection scheme proposed in [GDB+11] for SC-FDE systems. An analytical expression for the PER is derived there and briefly described in this section.
Nodes contend for the channel at each epoch and collisions might happen. A data block, of N symbols, transmitted by a user p and experiencing multiple collisions, can be expressed, on the time domain, as $\{s_{n,p}; n = 0, ..., N-1\}$, and its correspondent on the frequency domain as $\{S_{k,p}; k = 0, ..., N-1\}$. At the receiver, at the frequency domain, the received signal from multiple MTs for a given transmission r is

$$Y_k^{(r)} = \sum_{p=1}^{P} S_{k,p} H_{k,p}^{(r)} + N_k^{(r)}, \tag{3.1}$$

where $H_{k,p}^{(r)}$ is the channel response for the pth MT at the rth transmission. $N_k^{(r)}$ is the channel noise for the rth transmission. The total number of slots allocated to an epoch until the $l+1$th super-frame is given by ζ_l. Considering that P MTs transmit $P + \zeta_l$ times

and $0 \leq l \leq R$, then the received $P + \zeta_l$ transmissions are characterized as follows:

$$\begin{aligned} \mathbf{Y}_k &= \mathbf{H}_k^T \mathbf{S}_k + \mathbf{N}_k \\ &= \begin{bmatrix} H_{k,1}^{(1)} & \dots & H_{k,P}^{(1)} \\ \vdots & \ddots & \vdots \\ H_{k,1}^{(P+\zeta_l)} & \dots & H_{k,P}^{(P+\zeta_l)} \end{bmatrix} \begin{bmatrix} S_{k,1} \\ \vdots \\ S_{k,P} \end{bmatrix} + \begin{bmatrix} N_k^{(1)} \\ \vdots \\ N_k^{(P+\zeta_l)} \end{bmatrix} \end{aligned} \tag{3.2}$$

For a given MT p, the estimated signal at the frequency domain is

$$\tilde{S}_{k,p} = \begin{bmatrix} F_{k,p}^{(1)} & \dots & F_{k,p}^{(P+\zeta_l)} \end{bmatrix} \mathbf{Y}_k = \mathbf{F}_{k,p}^T \mathbf{Y}_k \, . \tag{3.3}$$

$\mathbf{F}_{k,p}$ corresponds to the feedforward coefficients of the proposed system, and these are chosen to minimize the mean square error $2\sigma_{E_{k,p}}^2$ for a MT p. Considering that $\mathbf{\Gamma}_p = [\Gamma_{p,1} = 0, \dots, \Gamma_{p,p} = 1, \dots, \Gamma_{p,P} = 0]^T$, $2\sigma_{E_{k,p}}^2$ is evaluated as follows

$$\begin{aligned} 2\sigma_{E_{k,p}}^2 &= \mathbb{E}\left[|\tilde{S}_{k,p} - S_{k,p}|^2 \right] \\ &= \left(\mathbf{F}_{k,p}^T \mathbf{H}_k^T - \mathbf{\Gamma}_p \right) \mathbb{E}\left[\mathbf{S}_k \mathbf{S}_k^H \right] \left(\mathbf{F}_{k,p}^T \mathbf{H}_k^T - \mathbf{\Gamma}_p \right)^H \\ &\quad + \mathbf{F}_{k,p}^T \mathbb{E}\left[\mathbf{N}_k \mathbf{N}_k^H \right] \mathbf{F}_{k,p}^* \, . \end{aligned} \tag{3.4}$$

Regarding $\mathbb{E}\left[|S_{k,p}|^2 \right] = 2\sigma_S^2$ and $\mathbb{E}\left[\left| N_k^{(r)} \right|^2 \right] = 2\sigma_N^2$, the optimal $\mathbf{F}_{k,p}$ is obtained by applying the method of Lagrange multipliers to (3.4), which results[1]

$$\mathbf{F}_{k,p} = \left(\mathbf{H}_k^H \mathbf{H}_k + \frac{2\sigma_N^2}{2\sigma_S^2} \mathbf{I}_{P+\zeta_l} \right)^{-1} \mathbf{H}_k^H \mathbf{\Gamma}_p \left(1 - \frac{1}{2N\sigma_S^2} \right) \, . \tag{3.5}$$

From (3.4) and (3.5) results

$$\sigma_p^2 = \frac{1}{N^2} \sum_{k=0}^{N-1} \mathbb{E}\left[\left| \tilde{S}_{k,p} - S_{k,p} \right|^2 \right] \, . \tag{3.6}$$

For a Quadrature Phase Shift Keying (QPSK) constellation and being $Q(x)$ the well known Gaussian error function, the Bit Error Rate (BER) of a given user p is

$$BER_p \simeq Q\left(\frac{1}{\sigma_p} \right) . \tag{3.7}$$

For an uncoded system with independent and isolated errors, the PER for a fixed packet size of M bits is

$$PER_p \simeq 1 - (1 - BER_p)^M . \tag{3.8}$$

[1] It should be noted that σ_s^2 and σ_N^2 denote the variance of the real and imaginary parts of $S_{k,p}$ and $N_k^{(r)}$ respectively.

3.3 Analytical Model

This section studies how the throughput, delay, jitter and energy consumption of a demand assigned uplink channel in a S-NDMA system are influenced by the PER, transmission power and the distance to the satellite. The following modeling conditions were considered:

a) The number of MTs transmitting in a slot, P, is known and follows the schedule defined by the satellite.

b) Perfect average power control, that leads to a uniform average E_b/N_0 value for all MTs at the satellite.

3.3.1 Packet Transmission

A packet is transmitted within an epoch, and the system behavior can be modeled by its state during the sequence of super-frames that belong to the epoch. For a demand assigned approach, the uplink schedule is defined by a slot vector $\mathbf{n} = [n_0, n_1, ..., n_R]$, which specifies how many redundant slots are allocated to the P MTs that transmit during an epoch (besides the initial P slots always defined), in up to a maximum of $R + 1$ super-frames.
For a scenario with perfect average power control, it is irrelevant which MTs stopped transmitting during each retransmission super-frame but not the number of MTs that stopped transmitting after a super-frame, due to a successful packet. The system state, denoted by the vector $\Psi^{(l)} = \{\psi_k^{(l)}, k = 0...l\}$, can be defined by the number of MTs whose packets were successfully received and stopped transmitting at the end of the super-frame $k = 0, ..., l$ (assuming $l \leq R$ retransmission super-frames exist during an epoch). The random variables $\psi_k^{(l)}$ satisfy

$$\sum_{k=0}^{l} \psi_k^{(l)} = P \ , \tag{3.9}$$

for all $l \in [0, R]$, since the total number of MTs transmitting during the epoch is equal to P.
The state space of $\Psi^{(l)}$ is an $l + 1$-dimension Pascal's simplex, denoted by the set $\Omega_P^{(l)}$, which has a finite number of values for a vector $K^{(l)} \in \Omega_P^{(l)}$ that satisfy equation (3.9). Each state $\Psi^{(l)} = \{\psi_0^{(l)} = K_0^{(l)}, ..., \psi_l^{(l)} = K_l^{(l)}\}$ defines the set of transmission sequences, $\varsigma\left(\Psi^{(l)} = K^{(l)}\right)$, where $K_0^{(l)}$ MTs stopped transmitting after the initial $P + n_0$ slots, $K_1^{(l)}$ MTs stopped transmitting after the first retransmission super-frame, and so on until $K_l^{(l)}$ MTs stopped transmission at the last retransmission super-frame considered, $l \leq R$. The cardinality of $\varsigma\left(\Psi^{(l)} = K^{(l)}\right)$ defines the total number of combinations of MTs transmissions that produce this transmission sequence, and is equal to the following multinomial

coefficient

$$\left|\varsigma\left(\Psi^{(l)}=K^{(l)}\right)\right|=\frac{P!}{\prod_{k=0}^{l}K_k^{(l)}!}\ . \tag{3.10}$$

The epoch ends when all packets are correctly received at the satellite, or after R retransmission super-frames. Therefore, the epoch is defined by $\Psi^{(R)}$.
The probability mass function for $\Psi^{(R)}$ can be defined recursively using the probability mass functions of $\Psi^{(l)}$ for $l=0,...,R$. All MTs transmit in the first super-frame, so $\Psi^{(0)}=P$ is constant.
The average packet error rate at the $l+1$th super-frame with P MTs is denoted by $PER_P\left(\Psi^{(l)}\right)$, and for the proposed receiver it is calculated using (3.3)-(3.8), where H_k is a $(P+\zeta_l)\times P$ matrix with the channel response. This matrix has zero coefficients for the slots of the epoch where the MTs did not transmit.
For a given E_b/N_0, the PER can be reduced by increasing the number of retransmissions of a packet. For the same number of retransmissions, the PER decreases when the number of interfering concurrent transmissions is also decreased. So, when a MT transmits $P+\zeta_l$ copies of a packet, the actual PER ($PER_l\left(\Psi^{(l)}\right)$) is bounded by

$$PER_l\left(\Psi=[P-1,0,...,1]\right)\leq PER_l\left(\Psi^{(l)}\right)\leq PER_l\left(\Psi=[0,0,...,P]\right)\ , \tag{3.11}$$

where PER_l corresponds to the average PER of the users that transmit at the $l+1$th super-frame.
At the end of a super-frame $l+1$, MTs with packets not received by the BS retransmit them at the next super-frame; the MTs that transmitted successfully at super-frame $l+1$ will be counted by $\psi_l^{(x)}$ for $x=l+1,...,R$. The conditional probability mass function for $\psi^{(l+1)}$ given $\psi^{(l)}$ follows

$$\begin{aligned}Pr\Big\{\Psi^{(l+1)}=\Big[&\psi_0^{(l+1)}=K_0^{(l)},...,\psi_{l-1}^{(l+1)}=K_{l-1}^{(l)},\\&\psi_l^{(l+1)}=m,\psi_{l+1}^{(l+1)}=K_l^{(l)}-m\Big]\mid\Psi^{(l)}=K^{(l)}\Big\}\\&=bi\left(K_l^{(l)},m,1-PER_l\left(\Psi^{(l)}\right)\right)\ ,\end{aligned} \tag{3.12}$$

where $bi(J,k,p)=\binom{J}{k}(1-p)^{J-k}$ denotes the binomial distribution and $\psi_l^{(l+1)}=n\in\left[0,K_l^{(l)}\right]$ represents the number of packets successfully received during retransmission super-frame l. Equation (3.12) can be used to generate all possible values of $K^{(R)}$ in $\Omega_P^{(R)}$, by exploring all valid l and n values. The probability mass function for $\Psi^{(l)}$ can also be

written explicitly as

$$Pr\left\{\Psi^{(l)} = K^{(l)}\right\} = \frac{P!}{\prod_{k=0}^{l} K_k^{(l)}!}\left(\prod_{i=0}^{l} PER_i\left(\Psi^{(i)}\right)\right)^{K_l^{(l)}} \prod_{j=0}^{l-1}\left(\left(1 - PER_j\left(\Psi^{(j)}\right)\right)\prod_{i=0}^{j-1} PER_i\left(\Psi^{(i)}\right)\right)^{K_j^{(l)}}, \tag{3.13}$$

where

$$\psi_j^{(i)} = \begin{cases} \psi_j^{(l)} = K_j^{(l)} & j < i < l \\ \psi_i^{(i)} = \sum_{k=i}^{l} K_k^{(l)} & j = i < l \end{cases}. \tag{3.14}$$

The average number of slots used by a MT to transmit a packet during an epoch with P active MTs where $\Psi^{(R)} = K^{(R)}$ is

$$tx\left(\Psi^{(R)} = K^{(R)}\right) = \frac{1}{P}\sum_{l=0}^{R}(P + \zeta_l)K_l^{(R)}. \tag{3.15}$$

The expected number of slots can be calculated using a Bayesian approach for all $K^{(R)}$ in $\Omega_P^{(R)}$,

$$\mathbb{E}\left[tx\left(\Omega_P^{(R)}\right)\right] = \sum_{K^{(R)}\in\Omega_P^{(R)}} Pr\left\{\Psi^{(R)} = K^{(R)}\right\} tx\left(\Psi^{(R)} = K^{(R)}\right). \tag{3.16}$$

A packet is not correctly received if it is transmitted on all epoch slots and its reception fails after the last slot. Consequently, the expected number of packets received with errors during an epoch is

$$\mathbb{E}\left[err\left(\Psi^{(R)} = K^{(R)}\right)\right] = K_R^{(R)} PER_R\left(\Psi^{(R)}\right). \tag{3.17}$$

Assuming that packet failures are independent, the packet error probability for an epoch $\Omega_P^{(R)}$ is given by

$$p_{err}\left(\Omega_P^{(R)}\right) = \sum_{K^{(R)}\in\Omega_P^{(R)}} \frac{1}{P} Pr\left\{\Psi^{(R)} = K^{(R)}\right\}\mathbb{E}\left[err\left(\Psi^{(R)} = K^{(R)}\right)\right]. \tag{3.18}$$

An upper bound for the packet error probability of an epoch with R retransmission

super-frames can be calculated using (3.11),

$$p_{err}\left(\Omega_P^{(R)}\right) \leq PER_R\left(\Psi^{(R)} = [0, 0, ..., P]\right) . \tag{3.19}$$

3.3.2 Transmission Parameters

A communication link between a MT and a satellite requires the definition of a set of Radio Frequency (RF) link parameters: p_t = transmitted power (Watts); p_r = received power (Watts); g_t = transmit antenna gain; g_r = receive antenna gain; and r_s = path distance (meters).
The antenna's transmission power of an handheld MT is a parameter that has some limitations, due to people safety concerns. Therefore, it was decided to fix p_t with a value of 2.5 Watts, aligned with current handheld MTs.
Beyond the fixed p_t value, it is necessary to obtain the values of g_t, g_r and the free space path loss lfs, in order to calculate the power received in satellite (p_r). According to [Jr.08], the antennas gains are given by

$$g = \eta_a \left(\frac{\pi d_m}{\lambda}\right)^2, \tag{3.20}$$

where η_a corresponds to the antenna aperture efficiency, d_m indicates the antenna's physical diameter, and λ the wavelength in the free space. As the λ value can be given by

$$\lambda = \frac{c}{f_c}, \tag{3.21}$$

where c is the phase velocity of light in a vacuum, and f_c is carrier wave frequency. So the gain equation can be simplified to

$$g = 109.66 f^2 d_m^2 \eta_a. \tag{3.22}$$

The gain equation is used to calculate g_t and g_r, varying only the antennas diameters, and it was assumed a diameter of $0.1m$ to the MT antenna, a diameter of $2.1m$ for the satellite antenna and an aperture efficiency of 90% was considered for both antennas. The carrier wave frequency was stipulated as f_c = 2.2 GHz, which is situated in *L band*. According to [Jr.08] the gains of both antennas in dBs are given by

$$G = 10 log_{10}(109.66 f_c^2 d_m^2 \eta_a), \tag{3.23}$$

so it results in an MT antenna gain of $G_T = 6.7914 dBs$ and in a satellite antenna gain of $G_S = 33.2357 dBs$.
According to [Jr.08] the equation that calculates the free space path loss in dBs (L_{fs}) is given by

$$L_{fs} = 20 \log(f_c) + 20 \log(r_s) + 92.44, \tag{3.24}$$

where r_s is variable, by taking into account the different positions of satellites, and f_c is in GHz. After all these parameters are calculated and considered, and having p_t as the transmitted power in dBs, it is possible to calculate the received power, which according to [Jr.08], it is calculated as follows,

$$P_r(dB) = p_t + G_T + G_S - L_{fs}. \tag{3.25}$$

These transmission/reception parameters are always considered during the communication between MTs and satellites, and they are applied in this chapter, that analyse the comparison between S-NDMA and H-NDMA for a fixed $r_s = 780km$, and in the next chapter, where r_s is variable, due to the consideration of the satellites' movement.

3.3.3 Throughput

The throughput can be calculated using (3.26), where the ratio of the number of packets received per epoch to the average number of transmissions is calculated.

$$S = \frac{\sum_{j=1}^{P} j \; bi\left(P, j, 1 - p_{err}\left(\Omega_P^{(R)}\right)\right)}{\mathbb{E}\left[tx\left(\Omega_P^{(R)}\right)\right]}. \tag{3.26}$$

3.3.4 Packet Service Time

The packet's service time, τ_s, depends mainly on which super-frame of an epoch the packet is correctly received, but is also affected by scheduling delay relatively to the previous slots. Its expected value when P MTs transmit in an epoch can be defined as

$$\begin{aligned}
\mathbb{E}\left[\tau_s\right] &= \left(RT + n_R\delta + \mathbb{E}\left[\epsilon_R\right]\right) \prod_{i=0}^{R} p_{err}\left(\Omega_P^{(i)}\right) + \\
&\left(\sum_{r=0}^{R} \left(rT + n_r\delta + \mathbb{E}\left[\epsilon_r\right]\right)\left(1 - p_{err}\left(\Omega_P^{(r)}\right)\right) \prod_{i=0}^{r-1} p_{err}\left(\Omega_P^{(i)}\right)\right) \\
&\approx \left(\sum_{r=0}^{R} \left(rT + n_r\delta\right)\left(1 - p_{err}\left(\Omega_P^{(r)}\right)\right) \prod_{i=0}^{r-1} p_{err}\left(\Omega_P^{(i)}\right)\right) \\
&\quad + \left(RT + n_R\delta\right) \prod_{i=0}^{R} p_{err}\left(\Omega_P^{(i)}\right) + \mathbb{E}\left[\epsilon\right],
\end{aligned} \tag{3.27}$$

where ϵ_r denotes the scheduling delay for super-frame r and δ denotes the slot time duration. It is assumed the simplification that the scheduling delay statistics do not depends on the super-frame index, so that they can be modeled by a single random variable ϵ.

3.3.5 Energy Consumption

Multiple MTs transmit packets to the uplink channel, which arrive at the BS with an average reception power P_r due to the assumption of perfect average power control. A simplified energy model is proposed in this section, which considers only the transmission energy and neglects the energy consumption related to the circuit and algorithm complexity [SA05].

The transmission power per packet, P_p, for each MT includes the transmission signal power p_t and the amplifier's power consumption P_{amp}, where $P_{amp} = \beta p_t$. The transmission power per packet can be then defined as $P_p = (1+\beta)p_t$. β is given by $\beta = \xi/\eta - 1$ with η as the drain efficiency of the radio frequency power amplifier and ξ as the peak-to-average-ratio [SA05]. A constant value $\eta = 0.35$ was considered. For a QPSK constellation, $\xi \approx 15/2$, considering that the bandwidth efficiency is approximately equal to the number of bits per symbol for an Multi-Level Quadrature Amplitude Modulation (M-QAM) constellation [SA05].

Considering that E_b/N_0 is the bit energy E_b over the noise N_0 ratio, then the Additive White Gaussian Noise (AWGN) power spectral density is $\sigma_N^2 = \frac{N_0}{2} = -174$ dBm/Hz for a given bandwidth B; the energy for each packet transmission E_p is

$$E_p = (1+\beta)\, p_t T_{on} \tag{3.28}$$

assuming $P_r = \frac{ME_b}{T_{on}}$ and $E_p = P_p T_{on}$, where T_{on} is the packet transmission time for a total of M bits and p_t is the transmission power with a constant value of 2.5 Watts.

The energy per useful packet, denoted by $EPUP$, measures the average transmitted energy for each packet correctly received by the BS. It depends on the expected number of epochs required for the BS to receive correctly the packet, $E[N_\epsilon]$, the average energy consumption during each epoch, and the success rate at the end of the last epoch.

Considering that packet transmissions occur in up to M_E successive epochs, the success rate is given by $1-(P_{err})^{M_E}$, where P_{err} denotes the average packet error probability during an epoch, given by (3.18). Therefore, the average number of epochs to transmit a packet with success is

$$\begin{aligned}\mathbb{E}[N_\epsilon] &= \sum_{k=0}^{M_E-1} (k+1)\,(P_{err})^k\,(1-P_{err}) + M_E\,(P_{err})^{M_E} \\ &= 1-(P_{err})^{M_E} + P_{err}\frac{1-(P_{err})^{M_E}}{1-P_{err}}\,.\end{aligned} \tag{3.29}$$

The average number of slots where the MT transmits during an epoch, $E[Tx_\epsilon]$, can be calculated using (3.16).

Finally, the Energy per Useful Packet transmission ($EPUP$) is given by

$$EPUP(P, R, M_E, E_b/N_0) = \frac{\mathbb{E}\left[N_\epsilon\right] E\left[Tx_\epsilon\right] E_p}{\left(1 - (P_{err})^{M_E}\right)} \ . \tag{3.30}$$

3.3.6 QoS Constraints

Satellite networks' RTT presents major challenges when QoS guarantees have to be provided to multimedia traffic. For a given QoS class these constraints typically include the specification of [AMCV06] an upper PER threshold (PER_{max}) and delay bound (D_{max}). The objective should be to minimize the EPUP and to provide these guarantees supporting the total traffic load $\lambda = \sum_{p=1}^{P} \lambda_p$, which comprehends the load coming from all the P MTs connected to the satellite. A final concern relates to the different distances from the satellite to each MT; a farther away MT requires higher transmission power, which might origin different coverage regions of a satellite depending on the QoS class. In the analysis done here it is assumed that only MTs at similar distances to the satellite are grouped into an epoch. Thus, the epoch's $EPUP$ optimization takes only into account the number of MTs transmitting and not the distance to the satellite.

The system's performance is influenced by the scheduled number P of MTs in an epoch and the average E_b/N_0 measured at the satellite. Using the model proposed above, it is possible to predict how the system behaves for all possible values for P and E_b/N_0, and to define the optimal values for the S-NDMA parameters taking into account the QoS requirements.

When a PER_{max} bound requirement is defined, it is necessary to calculate the minimum number of packet transmissions, $\zeta_R + P$, that guarantee it. It is clear that $\mathbf{H}_k^T$ in (3.3) is not affected when R is set to zero or a value above zero, as long as the total number of slots with transmissions ($\zeta_0' + P$ for a single super-frame) does not change, i.e. $\zeta_0' = \zeta_R$. From (3.19), ζ_R could be obtained as the minimum value of $\zeta_0' = n_0'$ that satisfies the condition,

$$\zeta_R \approx \min_{n_0'} \left\{ PER_0\left(\Psi'^{(0)} = [P]\right) \leq PER_{max} \right\} \ . \tag{3.31}$$

A D_{max} delay bound introduces a limitation in the number of super-frames that can be part of an epoch. The dominant component of (3.27) is due to the product RT, where T depends on the altitude of the satellite orbits (e.g. $T \approx 154.8$ ms for a MEO with an altitude of 23222 km and $T \approx 5.2$ ms for a LEO satellite network with an altitude of 781 km, considering an angle of $0\,^\circ$). Assuming that no error recovery is tried after an epoch, i.e. $M_E = 1$, R must satisfy

$$R \leq 1 + \lfloor D_{max}/T \rfloor \ , \tag{3.32}$$

where $\lfloor x \rfloor$ defines the floor operation, that returns the maximum integer below or equal to x. Given R, it is necessary to define the vector $\mathbf{n}$, which specifies how the ζ_R slots

are distributed over the $R+1$ super-frames. This problem can be defined as an $EPUP$ minimization problem, since the condition above already insures the delay bound,

$$\mathbf{n}^{\star} = \min_{\mathbf{n}} \{EPUP(P, R, 1, E_b/N_0)\} \ . \tag{3.33}$$

On the other hand, for the QoS classes that do not define a delay bound, it is trivial to prove that the lowest $EPUP$ is achieved when $\mathbf{n} = [0, 1, 1, ..., 1]$, which corresponds to the transmission pattern used in H-NDMA. In this case, M_E can be above one, to allow having assured packet transmissions with bounded epoch durations.
These set of equations can be used to define the optimal parameters for S-NDMA transmissions, which can be formulated as:

$$\begin{aligned} \text{Minimize:} \quad & EPUP\left(P^{\star}, E_b^{\star}/N_0\right) \\ \text{Subject to:} \quad & S < 1 \ , \\ & S \geq J\lambda \ , \\ & \mathbb{E}\left[\tau_s\right] \leq D_{max} \ . \end{aligned}$$

This research work intends to evaluate the feasibility of such parameter selection algorithm. The next section, analyzes the S-NDMA performance for different QoS requirements, for different P, E_b/N_0 and $\mathbf{n}$ values, and compares it with the performance of H-NDMA.

3.4 Performance Analysis

In this section, the system performance is analyzed for H-NDMA and S-NDMA, considering the PER, throughput, EPUP and delay. It models an LEO satellite constellation, with circular orbits at an altitude of 781 km (like in Iridium). In these conditions, we define T based on the RTT of the furthest MT within a coverage range of 1720 km radius (corresponding to $30\,^{\circ}$ of the earth's perimeter, requiring a minimum of six satellites per orbit and six orbit planes to provide full coverage of the earth's surface).

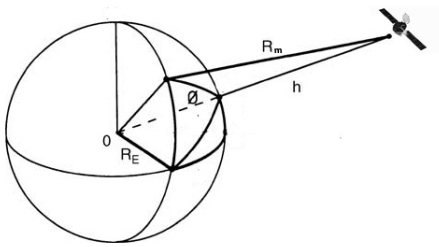

Figure 3.3: Satellite with θ displacement for RTT calculation purposes

Figure 3.3 illustrates the way RTT was calculated for $\theta = 30\,^{\circ}$. The earth's radius is

$R_{earth} = 6371$ km and the distance from earth surface to satellite H with $\theta = 0\,^{\circ}\mathrm{C}$ is 781 km. The distance from earth surface to satellite with $\theta = 30\,^{\circ}$, R_m is given by,

$$R_m = \sqrt{R_e^2 + (R_e + H)^2 - 2R_e(R_e + H)\cos\theta}.. \tag{3.34}$$

Using (3.34), it was possible to conclude that $R_m = 3580.4$ km for $\theta = 30^{\text{o}}$. Finally, the RTT to that distance is calculted using

$$RTT = 2 \times \frac{R_m}{c} \tag{3.35}$$

resulting $RTT = 23.8ms$.

A severely time dispersive channel was considered, with rich multipath propagation and uncorrelated Rayleigh fading for each path and user (similar results were obtained for other fading models). To cope with channel correlation for different retransmissions, the Shifted Packet technique of [DMB+09] was considered, where each retransmitted block has a different cyclic shift. MTs transmit uncoded data blocks with $N = 256$ symbols selected from a QPSK constellation with Gray mapping with a $4\mu s$ transmission time.

As an example, we consider video telephony traffic QoS requirements [AMCV06], which define a $PER_{max} \leq 1\%$ and $D_{max} \leq 100$ms. Due to the complexity of resolving (3.4) and (3.3) in real-time, the capacity to handle MPR is limited to a maximum value of $P+\zeta_R$. For this analysis it is considered a maximum number of 5 simultaneous MTs' transmissions and a value of $\zeta_R \leq 6$.

The S-NDMA configuration follows section 3.3.6. First, it is determined the minimum value of ζ_R that satisfies equation (3.31) for an average $PER \leq PER_{max}$, labelled in Figure 3.4 as ζ_{Rmax} for $P = 5$ MTs when E_b/N_0 is between -3 dB and 12 dB. The figure also represents the minimum value of ζ_R that allows an average $PER \leq 0.99$, which defines the minimum value that n_0 may take. The figure shows that it is possible to satisfy the PER condition for $E_b/N_0 \geq -2$dB with five transmitting MTs ($P = 5$). A lower number of MTs demand for higher E_b/N_0 values to satisfy the PER requirement. Given the D_{max} condition, M_E was set to one (no recovery from transmission failures during an epoch) and R was set to 3, guaranteeing that the maximum delay for any packet is within the defined D_{max} bound, even when an additional RTT is required to schedule the packet transmission. In order to find the optimal value for $\mathbf{n}$ that minimizes the $EPUP$, all possible values of $\mathbf{n}$ were tested to satisfy $n_0 \geq \zeta_{Rmin}$. Figure 3.5 depicts the values of $(EPUP/E_p)(E_b/N_0)$ for S-NDMA over n_1 and n_2 for $P = 5$ and $E_b/N_0 = -2$dB. For each individual MT, $(1/E_p)(E_b/N_0)$ is constant, given by (3.28). Therefore, $(EPUP/E_p)(E_b/N_0)$ shows the variation of $EPUP$, ignoring all individual MT specific parameters (path loss model, etc.). Figure 3.5 also depicts the minimum value achievable for H-NDMA. The figure shows that the $EPUP$ for $\mathbf{n}^\star$ is only slightly higher than the minimum $EPUP$ that could be achieved for H-NDMA. The remaining results presented below show the performance of S-NDMA for $\mathbf{n} = \mathbf{n}^\star$, which was calculated for all integer

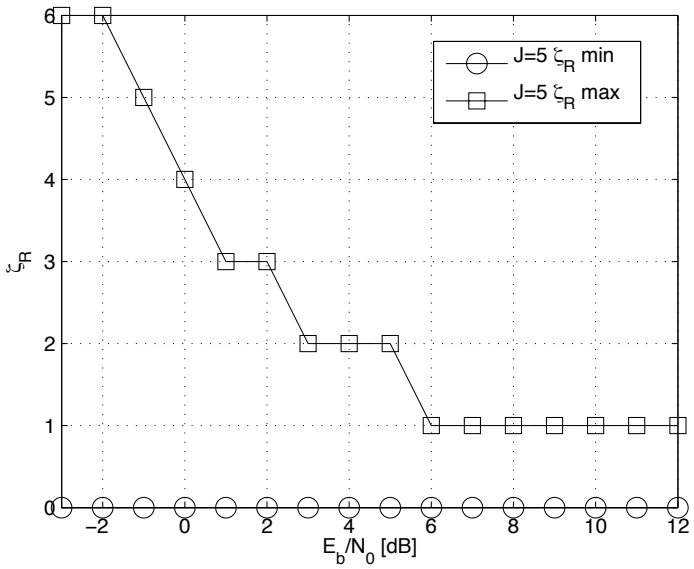

Figure 3.4: ζ_R maximum (satisfying PER_{max}) and minimum (satisfying $PER \leq 99\%$) over E_b/N_0 for $P = 5$ MTs.

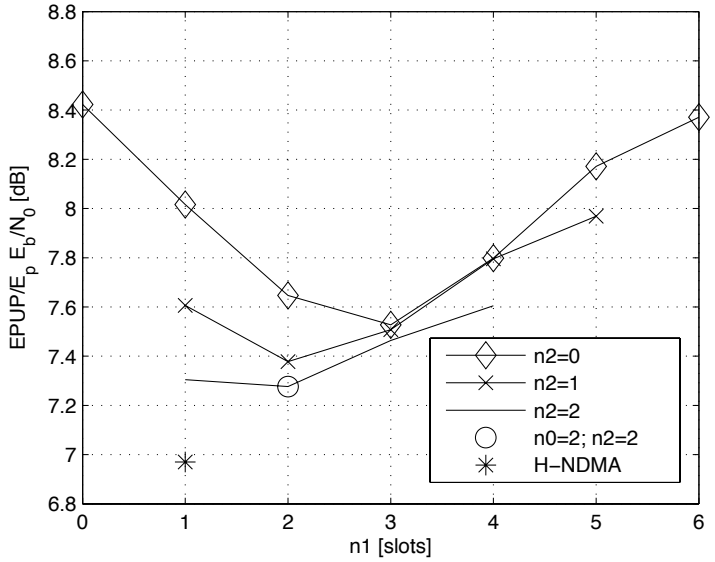

Figure 3.5: $(EPUP/E_p)(E_b/N_0)$ for varying $\mathbf{n}$ over n_1 for $E_b/N_0 = -2$dB and $P = 5$ MTs.

values of E_b/N_0 between -3 dB and 12dB and for one up to five transmitting MTs.

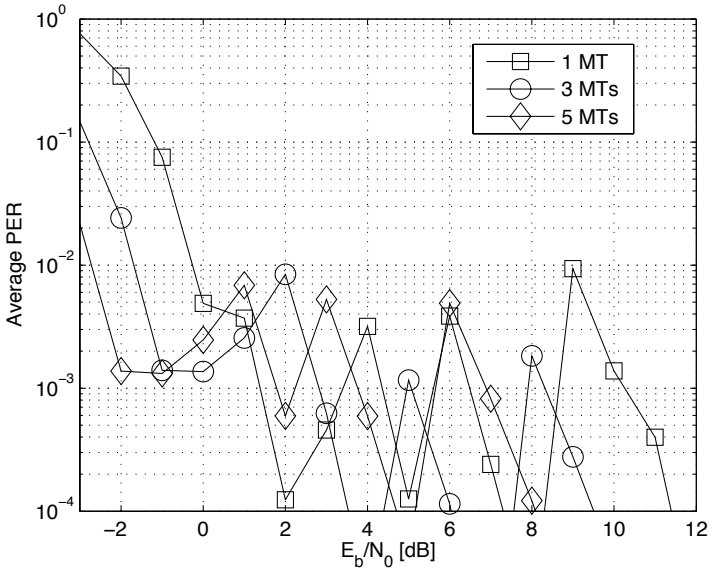

Figure 3.6: Average PER over E_b/N_0 and P for S-NDMA and H-NDMA.

Figure 3.6 depicts the average PER over E_b/N_0 and P for S-NDMA and H-NDMA, using the ζ_R value defined by (3.31). It shows that the Average PER condition is satisfied by all scenarios tested for $E_b/N_0 > 0$dB, and for $E_b/N_0 > -2$dB for $P = 5$MTs. The irregular pattern of the average PER is due to the variation of the total number of slots used to transmit a packet, represented by ζ_{Rmax} in figure 3.4. Figure 3.7 depicts the saturated throughput, calculated using (3.26), for different P and E_b/N_0 values and for H-NDMA and S-NDMA. The figure shows that the system throughput increases with higher P values (i.e. with more MTs transmitting). It also shows that S-NDMA's throughput, compared to H-NDMA's, degrades for higher P values for low E_b/N_0 values. For higher E_b/N_0 values the S-NDMA's throughput follows H-NDMA's since both systems are equivalent as $\zeta_R \leq 2$ and $\mathbf{n}^\star = [011]$ for S-NDMA. Figure 3.8 depicts the $(EPUP/E_p)(E_b/N_0)$ calculated using (3.30), in the conditions of figure 3.7. It shows that a higher number of MTs transmitting require a higher $EPUP$ for each packet transmitted, confirming that S-NDMA also slightly degrades the $EPUP$ compared to H-NDMA. However, since the throughput increment is more significant than the $EPUP$ degradation, a higher number of MTs actually decreases the average $EPUP$ measured for a given throughput level, represented in figure 3.9. This figure shows that the minimum $EPUP$ value for S-NDMA is reached for $P = 5$ MTs and $S \approx 53\%$, and that it grows for higher throughputs. Notice that this configuration also applies to lower throughput values, since idle slots can be introduced in the super-frame, to force a higher throughput in the remaining slots, as long as the number of scheduled MTs is at least five.

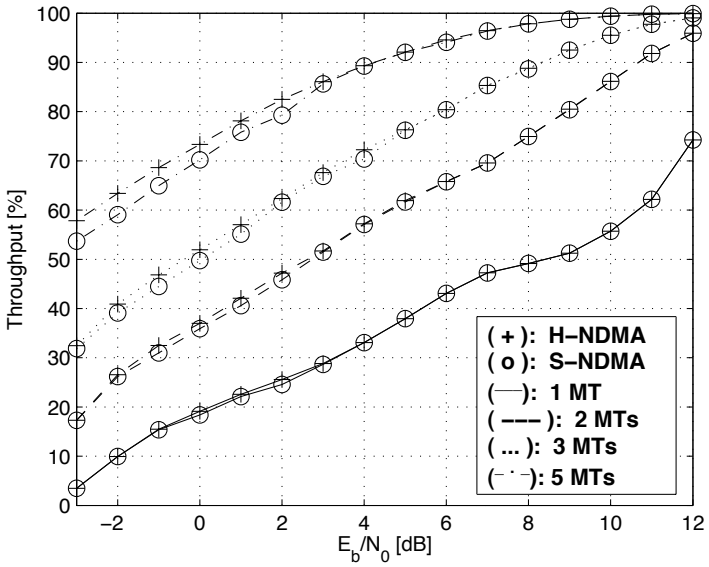

Figure 3.7: Saturated throughput over E_b/N_0 for $P = 5$ MTs for S-NDMA and H-NDMA.

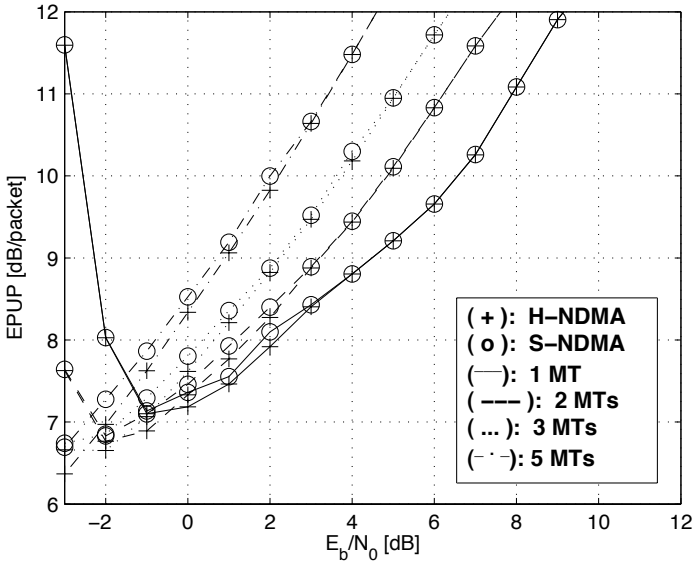

Figure 3.8: $(EPUP/E_p)(E_b/N_0)$ over E_b/N_0 and P for S-NDMA and H-NDMA.

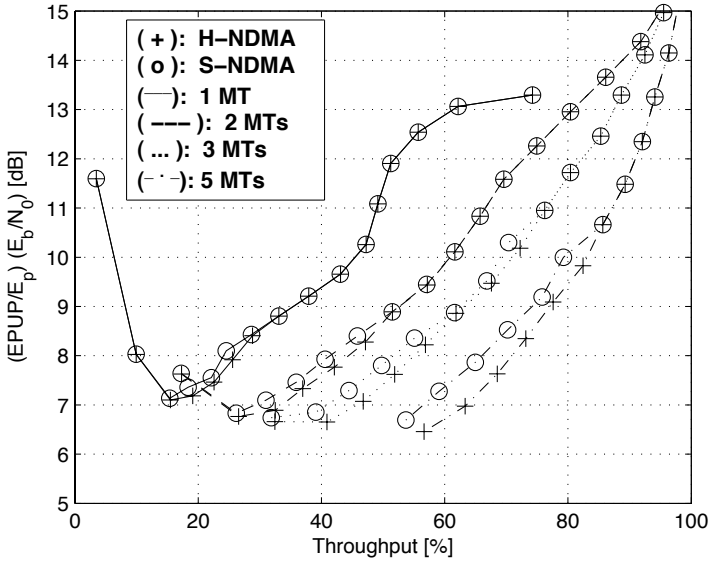

Figure 3.9: $(EPUP/E_p)(E_b/N_0)$ over Throughput (S) and P for S-NDMA and H-NDMA.

Figure 3.10 depicts the E_b/N_0 values that correspond to the $EPUP$ values represented in figure 3.9. The values represented can be used to define the E_b/N_0 value at the satellite for a given set of packets scheduled for transmission in a given slot. Using (3.25) and (3.28), the calculated E_b/N_0 value can be converted in the individual p_t value that each individual MT should use. The introduction of QoS requirements in S-NDMA forces an increment that may reach about 1 dB in the E_b/N_0 compared to a best effort minimum $EPUP$ approach, provided by H-NDMA.

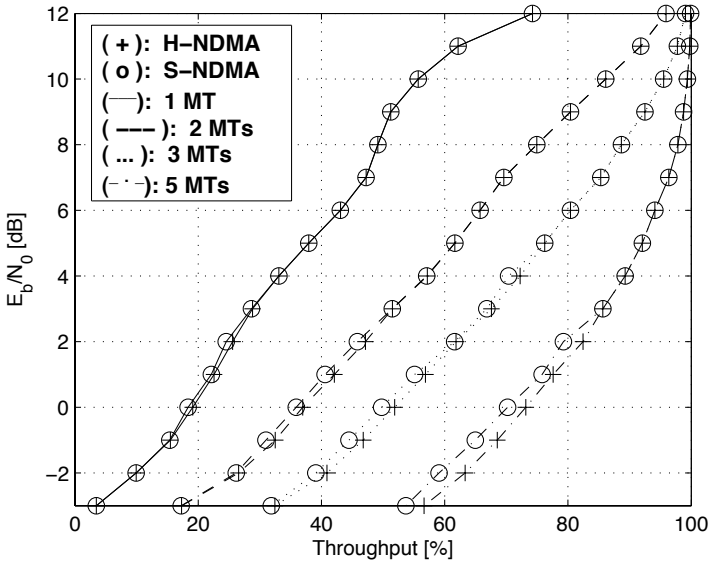

Figure 3.10: E_b/N_0 over Throughput (S) and P for S-NDMA and H-NDMA.

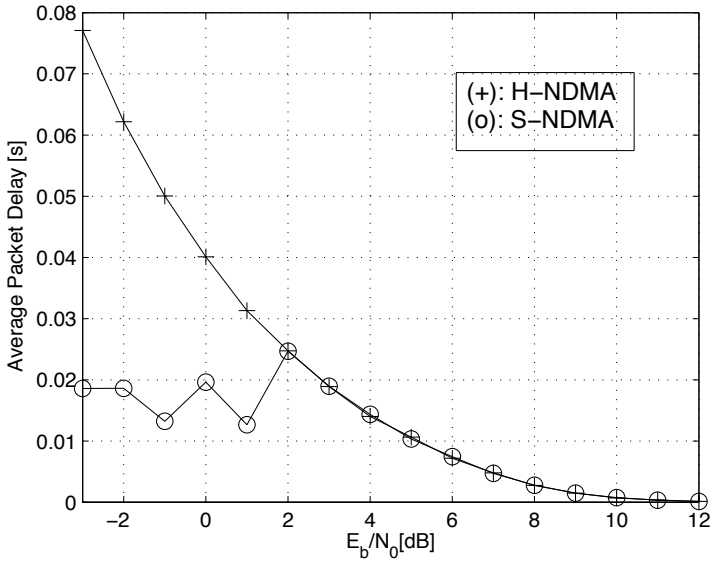

Figure 3.11: Average packet delay over E_b/N_0 for $P = 5$ MTs.

Figure 3.11 depicts the average packet delay over E_b/N_0 for $P = 5$ MTs for S-NDMA and H-NDMA. It can be seen that S-NDMA effectively controls the maximum delay, compared to H-NDMA, producing only a slight degradation in the energy per packet, illustrated in figure 3.9 for the most energy efficient network configuration. Therefore, S-NDMA can be used in a satellite network to provide QoS guarantees with measurable energy savings.

4

Satellite Handover

This chapter presents a new approach to the communication between MTs and satellites based on previous chapter (3) S-NDMA proposal. It is introduced the distributed multipacket reception communication with more than one satellite, allowing the study of alternative satellite handover processes. Two satellite handover schemes are illustrated, studied and discussed on this chapter. One of them consists in an intra-planar handover scheme, which is not based in a real LEO constellation, and the other one is based on the Iridium satellite constellation handover scheme. Optimal handover conditions are approached in this study, and issues like Doppler deviation and time offset due to satellite movement are analysed too. Throughput, energy consumption and packet delay analysis are present in this chapter too, considering the same QoS constraints assumed in the 3rd chapter.

4.1 Communication with Two Satellites

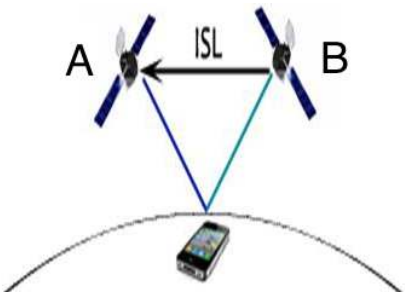

Figure 4.1: Basics of the communication with two satellites

Usually, a MT is associated to a single satellite and communicates only with that satellite. However, near the handover zones, the signal transmitted to the satellites can be received and processed by more than one satellite. This brings the possibility of using the signal received in other satellites to improve the communication during handover: it allows a soft handover approach with minimal service interruption and energy, when a distributed multipacket reception algorithm is used.

Figure 4.1 illustrates a communication between a MT and two satellites. The terminal sends a signal for both satellites, but it is only synchronized with the nearest one. For instance, the dark blue line on 4.1 represents the communication with the satellite that is closer, so the terminal and the satellite are synchronized through that link. The cyan line represents the communication channel with the farthest satellite. It is proposed the use of the Inter Satellite Link (ISL) to support the distributed MPR and satellite soft handover. The nearest satellite receives channel state information from the farthest satellite. Using this information it can combine the signal that comes from the MT and the other that comes from the other satellite through an ISL, represented in figure 4.1.

4.1.1 Multipacket Detection Receiver Structure

The communication with two satellites, implies some changes in multipacket detection receiver structure. Those differences are explained in relation to a single satellite communication structure, which is presented in section 3.2.2.

$$\begin{aligned} \mathbf{Y}_k &= \mathbf{H}_k^T \mathbf{S}_k + \mathbf{N}_k \\ &= \begin{bmatrix} H_{k,1}^{(1,1)} & \dots & H_{k,P}^{(1,1)} \\ \vdots & \ddots & \vdots \\ H_{k,1}^{(P+\zeta_l,1)} & \dots & H_{k,P}^{(P+\zeta_l,1)} \\ H_{k,1}^{(1,2)} & \dots & H_{k,P}^{(1,2)} \\ \vdots & \ddots & \vdots \\ H_{k,1}^{(P+\zeta_l,2)} & \dots & H_{k,P}^{(P+\zeta_l,2)} \end{bmatrix} \begin{bmatrix} S_{k,1} \\ \vdots \\ S_{k,P} \end{bmatrix} + \begin{bmatrix} N_k^{(1,1)} \\ \vdots \\ N_k^{(P+\zeta_l,1)} \\ N_k^{(1,2)} \\ \vdots \\ N_k^{(P+\zeta_l,2)} \end{bmatrix} \end{aligned} \tag{4.1}$$

It is possible to verify in equation (4.1) that the size of matrix H_k changed from equation (3.3), having now the double of lines. This change is related to the concatenation of channel state information measured locally and the channel state information received from the second satellite; it now combines spatial diversity and temporal diversity. An equal size change occurs in the N_k matrix, where the channel noise is measured, taking into account the communication with both satellites. The new lines present in H_k matrix are influenced by the different path losses on different satellites. This difference was mapped into the channel gain of the H_k coefficients associated to the second satellite. The average ratio of channel gains of the first and second satellites is given by $\sqrt{\frac{\frac{E_b^{(1)}}{N0}}{\frac{E_b^{(2)}}{N0}}}$.

The estimation of the signal at the frequency domain was also modified . Equation (3.3) changed by having twice the number of feedforward coefficients due to the additional signals from the second satellite. The new estimated signal at the frequency domain is given by

$$\tilde{S}_{k,p} = \left[F_{k,p}^{(1)} \quad ... \quad F_{k,p}^{(2(P+\zeta_l))} \right] \mathbf{Y}_k = \mathbf{F}_{k,p}^T \mathbf{Y}_k \ . \tag{4.2}$$

The rest of the Multipacket Detection Receiver Structure follows what was explained in 3.2.2 section.

Spatial diversity is present on this scheme, due to the reception of the signal in different antennas, for a subsequent signal combination. This process results in an improved signal reception with diversity gain.

4.1.2 Packet Transmission for Two Satellites

The packet transmission for two satellites is identical to packet transmission for a single satellite 3.3.1; the MT transmits according to what is specified in S-NDMA. The only difference is on the measured average packet error, which is lower due to the combination of two signals received in two satellites. The PER calculation at the $l+1$th super-frame with P MTs, $PER_P\left(\Psi^{(l)}\right)$ involves new H_k, having in this case a size of $(2(P+\zeta_l)) \times P$, which is the double of the lines of H_k in the communication with one satellite. The efficiency of this scheme depends on the satellite orbits adopted, and on how different are the time and frequency shifts. The next sections study these effects and the optimization of the proposed handover approach for two satellite orbits: considering handover within planar orbits; and considering the inter-satellite handovers used in the Iridium system.

4.2 Intra-planar Handover Scheme

Figure 4.2 illustrates a communication with two satellites, where both satellites move with the same speed in the same plan, so the distance between them does not change with the time or with the movement (it is equal to 5991,3 km). In the following analysis, it is considered that the terminal travels the earth surface following the velocity of the satellite's spots and the satellites are stopped. Seven satellites equally spaced are considered in a orbit that covers all the perimeter of the earth. The angle θ, measured from the centre of the Earth, between two satellites, (as it is indicated in figure 4.2), has a value of approximately $51.43\,^\circ$. The seven satellites were chosen by taking into consideration the maximum angle that a terminal in earth's surface can communicate with a satellite (approximately $54\,^\circ$). This angle is given by the skylines on both sides of the globe, because they are obstacles to the communication between the MT and the satellite. So the seven satellites was the optimal choice, because the θ angle is closer but smaller than $54\,^\circ$.

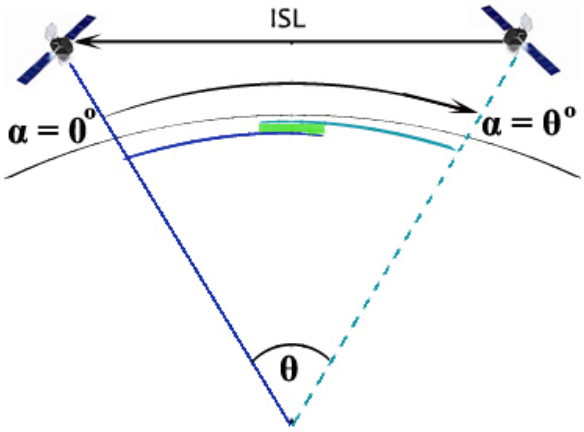

Figure 4.2: Intra-planar Handover Scheme

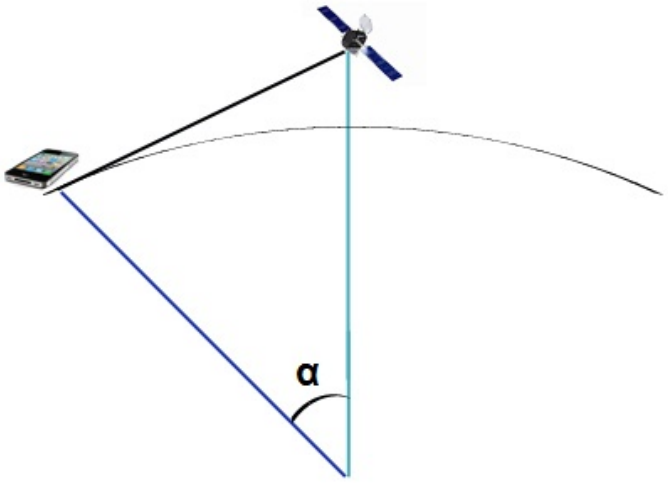

Figure 4.3: Maximum satellite range

The arrow right above the earth's surface in figure 4.2, indicates the path taken by the terminal (i.e. the satellites footprint) starting in $\alpha = 0\,^{\circ}$ and ending in $\alpha = \theta$. When the terminal starts the course, it only communicates with the satellite on the left side of the mentioned figure. When the value of α is equal to $0\,^{\circ}$, it is in the nearest point to the satellite. Due to the earth's shape and the satellite height considered (780) km, the terminal looses the satellite coverage when it reaches the skyline, for $\alpha_{max} = 27.03^{\circ}$, figure 4.3 illustrates the satellite maximum angle covered, and the largest distance where a terminal and a satellite are able to communicate. Considering figure 4.2, when α exceeds $27.03\,^{\circ}$, the terminal is only communicating with the satellite on the right side of

the figure. This satellite handover is usually not made abruptly; it is preceded by a zone where the terminal communicates with both satellites, which can be called the Handover Zone. As it is possible to see in figure 4.2, this handover zone is covered by both satellites during $2.68\,^{\circ}$, starting in $\alpha = 24.37\,^{\circ}$ and ending at $\alpha = 27.05\,^{\circ}$. The point on earth's surface where the terminal is equidistant to both satellites occurs when $\alpha = \frac{\theta}{2}$, in other words, when $\alpha = 25.71\,^{\circ}$. The handover zone for the second satellite is equal, with the same width of $2.68\,^{\circ}$. Due to the high orbital velocity of the satellite, the satellite crosses this handover zone in less than the RTT. Therefore, it is not possible to apply the H-ARQ approach while the MT is transmitting to two satellites during handover. The system has to be dimensioned to be successful with a single transmission burst. The use of a CDMA spreading factor $S_f = 128$, results in a transmission of a CDMA frame (figure 4.4) with 256 CDMA data blocks, where each CDMA data block has 128 chips and a overall duration of 4.26 ms, for a chip rate of 7.68 Mchips/s. By having this frame structure, it is possible to obtain a maximum PER of 1% with a lower ζ_l. The satellites height in this scenario vary from 780 m to 3251.7 km, which are respectively when $\alpha = 0\,^{\circ}$ and $\alpha = 27.05\,^{\circ}$.

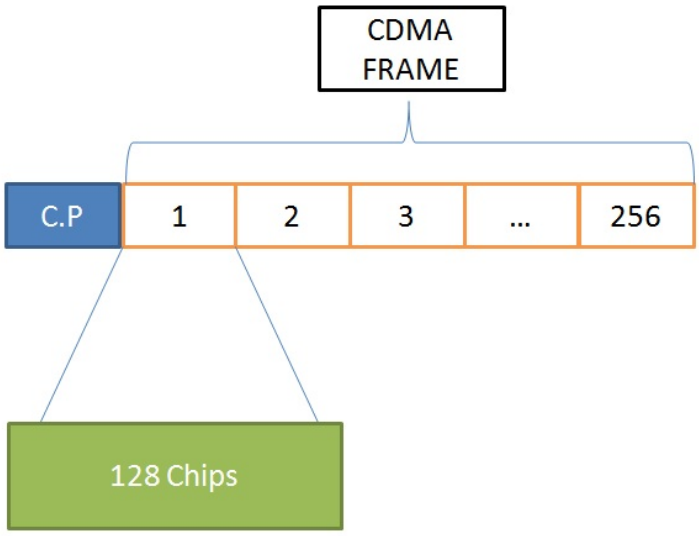

Figure 4.4: CDMA Frame

4.3 Iridium Handover Scheme

Iridium Handover scheme is studied as an example of a realistic vision of satellite handover process. This scheme takes into consideration the satellite coverage areas, also known as satellite footprints. The distance between adjacent cells center is $\sqrt{3}R_b$ [MAEIB12], where $R_b = 2209$km. The Iridium Handover was customized for this thesis purposes. Figure 4.5 represents the proposed handover scheme. Each circumference in figure 4.5 represents the coverage area of each satellite, having a radius R_b, equal to 2209Km. The

zones where the circumferences overlap, are the regions where the communication in parallel with more than one satellite occurs. As the satellites travels around the globe, these footprints are synchronously moving in relation to satellites, so it was decided for this analysis to also fix a point on earth's surface, and study the communication between the terminal and the satellites, while the footprints positions are changing. The cellphones line, depicted in figure 4.5, represents all the studied positions between the terminal and the satellite footprint. Regarding x axis, the footprints are moving towards decreasing values, so as the terminal is stopped or is moving with a much lower speed than the satellite, the position of the terminal relatively to the footprints evolves from bottom ($x = 0$) to top ($x = \frac{3}{2}R$) as it is represented by the arrow that stands next to the cellphones line.

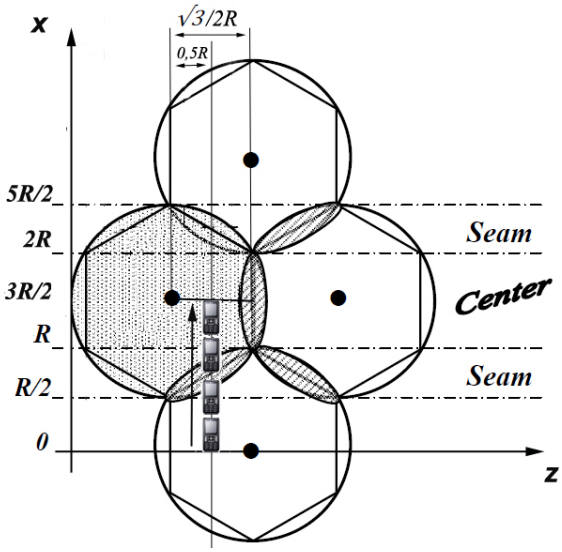

Figure 4.5: Iridium Handover Scheme

The figure 4.5 has four satellite footprints, but in this handover scheme, only two footprints are considered, which are the ones the illustrated cellphones line crosses. In other words, it is studied an handover between those two footprints, that are associated with two satellites. These two satellite footprints, along the cellphones line are represented by the following equations

$$MTPositions = \begin{cases} \left(x - \frac{3R_f}{2}\right)^2 + (z - R_f)^2 = R_f^2, \\ x^2 + \left(z - R_f + \frac{\sqrt{(3)}R_f}{2}\right)^2 = R_f^2, \\ z = 1.5R_f, \end{cases} \tag{4.3}$$

where R_f defines the satellite footprint radius; and z and x represent the figure 4.5 axis respectively. The distance between the two satellites on this scenario is constant, and is equal to 3826,1 km. The CDMA frame structure is equal to the one that was introduced on the previous scenario (figure 4.4).

4.4 Intra-planar Handover Scheme Performance Analysis

This section presents results concerning throughput, energy consumption, packet delay, Doppler deviation and time offset, for the intra-planar handover Scheme.

4.4.1 Doppler Deviation

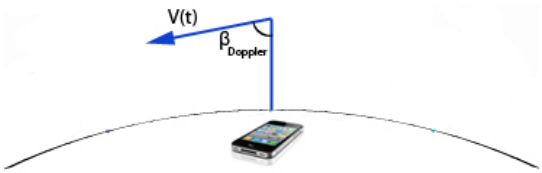

Figure 4.6: Doppler Deviation

Doppler deviation is characterized by the deviation on the original carrier frequency, due to fast-moving satellites. Actually the terminal present on earth's surface could be moving, but it can be considered that it is stopped, since its speed is much lower than the satellite speed. Figure 4.6 shows an arrow with a label $v(t)$, which represents the relative velocity between the satellite and the terminal. This relative velocity and its angle β with the signal propagation direction are used to obtain the value of the Doppler frequency shift, which is given by

$$f = f_c \left(1 + \frac{v(t)}{c} \cos(\beta)\right), \tag{4.4}$$

where f_c corresponds to original carrier frequency, and f to the frequency of the received signal, influenced by the Doppler shift. The figure 4.7 shows the evolution of the frequency of the received signal, by taking into account the satellite position α variation, and consequently β variation.

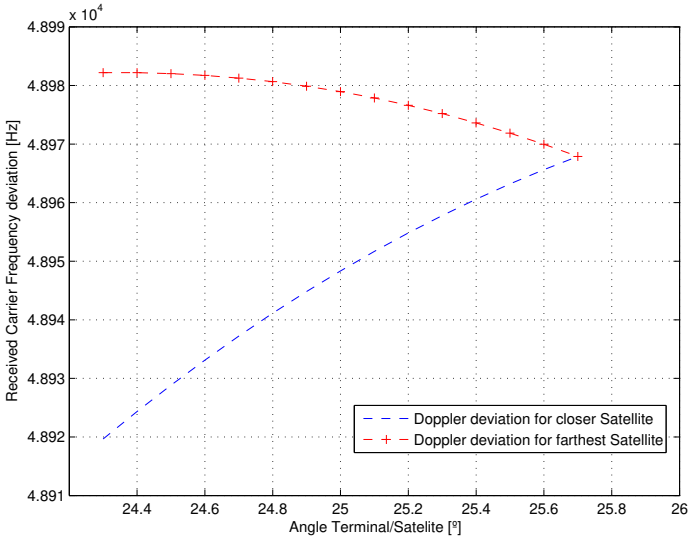

Figure 4.7: Doppler Deviation(α)

The carrier frequency considered is 2GHz, so the deviation is not significant, because it is much smaller when compared with the original frequency. Figure 4.7 presents the carrier deviation at the receiver. Only handover zone (communication with two satellites) was considered for this Doppler deviation study. In figure 4.2, when the terminal enters in the zone where it is covered by two satellites ($\alpha = 24.3\,°$), it is closer to the left satellite. Figure 4.6 shows that Doppler effect is less intense in the received carrier frequency for the closest satellite, and more intense on farthest satellite. It shows this effect from the point where the terminal enters the handover zone, until it is equidistant to both satellites, where the Doppler deviation is the same for both. A possible way to overlap this issue is by compensating on the receiver side that deviation, which is known *a priori*.

A way to compensate the Doppler offset is presented in [AMGL10], where the terminal continuously calculates the offset. After this calculation, the transmission of frequency is corrected in the opposite direction of Doppler deviation, so the transmitted carrier appears in the correct frequency at the receiver. This solution cannot be applied for the furthest satellite, since the transmitter already compensates the Doppler shift for the nearest satellite. A possible way to handle this shift is to compensate it at the receiver. When the satellite has several spot beams, it is possible to know *a priori* the deviation for each spot beam, which is a fraction of the deviation on the total footprint. Anyway, due to the low magnitude of this effect, it can mostly compensated by the SC-FDE transmission mechanism.

4.4.2 Time Offset

Beyond Doppler deviation, there is a time offset between the frame arrival instants in different satellites, since the distances paths among different satellites and the MT are

not the same. Therefore, when the terminal is communicating with two satellites, its transmission is only time aligned with the nearest one.

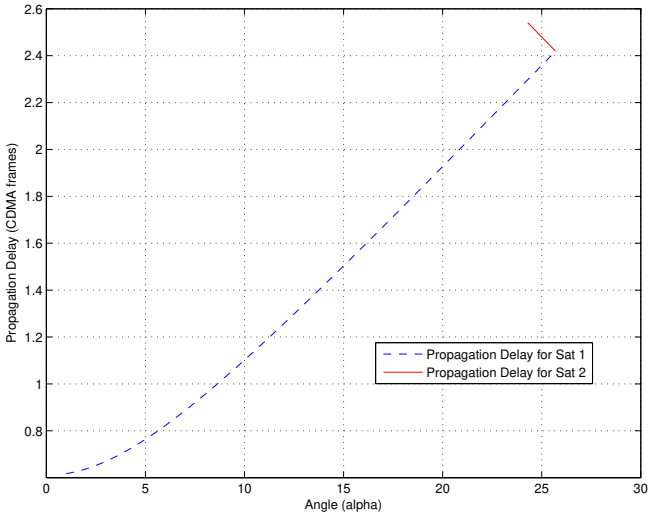

Figure 4.8: Propagation Delay (α)

Figure 4.8 depicts the propagation delay in the communication with the first satellite and with the second satellite, which will receive the MT after the handover.
One of the major advantages of SC-FDE is its capability of using low complexity frequency domain equalization instead of costly time-discrete convolution operations. This advantage is gained at the expense of a Cyclic Prefix (CP), which is necessary to cope with time dispersive channels. As with current OFDM-based (Orthogonal Frequency Division Multiplexing) schemes, the CP length is long enough to cope with the maximum relative channel delay. Therefore, it is well known that this time offsets can be compensated in a SC-FDE as long as they are shorter than the cyclic prefix duration. So, this CP can be made large enough to compensate the maximum signal delay associated to the satellites in the border of the coverage area, i.e, the satellites that can be involved in a handover process. Therefore in the worst case scenario (i.e handover between two satellites) the CP's size can be similar or higher than the size of a CDMA frame, which decreases the spectral efficiency of the system.
In this approach, the terminal has to do the handover in the part of the handover zone where the time shift is below the cyclic prefix. For instance, if a CP of approximately 20% of the size of a CDMA Frame is considered, when the MT enters the handover zone, it is capable of overlapping the propagation delay, because the difference between the propagation delay of both satellites is approximately 0.2 CDMA Frames. There is a trade-off between the time offset resilience and the bandwidth efficiency. So, we can reduce the handover zone, resulting in the decrease of approximately 10%, gaining bandwidth efficiency. For instance, it is possible to see in figure 4.8 that the time offset between the

communication with one and two satellites does not overlap the stipulated cyclic prefix duration when α is between ($25.2\,^{\circ}$) and ($25.7\,^{\circ}$), which would limit the handover to a subset of the handover zone ($0.5\,^{\circ}$). As the figure only represents half of terminal's travel, and the other part is symmetric, the terminal effective handover zone would be restricted to a course of ($1\,^{\circ}$). Another way to surpass this time offset constrain is by using conformal antennas [Jos06], which are antennas that are designed to follow a prescribed radiation pattern. They are composed by an array of several identical small antenna elements. In a receiving conformal antenna, the signals received by each antenna element are combined in the correct phase to enhance the signals from a specific direction and assures a bigger sensitivity to a signal that comes from a particular terminal. Conformal antennas give the possibility to generate two or more radiation beams, which can be better when compared to scanning a single beam. Again, using spot beams, it is possible to juxtapose several spots with a coverage of up to 1º, and to realign the frame structure at the receiver for each spot beam, guaranteeing that the time offset is bellow the cyclic prefix duration for the regions covered by each spot beam.

4.4.3 Throughput Analysis

Average throughput decreases with α's growth, because it leads to a larger distance between the terminal and the satellite. Figure 4.9 presents the throughput values from $\alpha = 0$ to the middle of handover zone (4.2). The throughput derivative from the communication with only one satellite is compared to the throughput on a communication with two satellites. During the handover zone, there is only communication with two satellites, but for better understanding, it was decided to show how the throughput with a single satellite would be on that zone too.

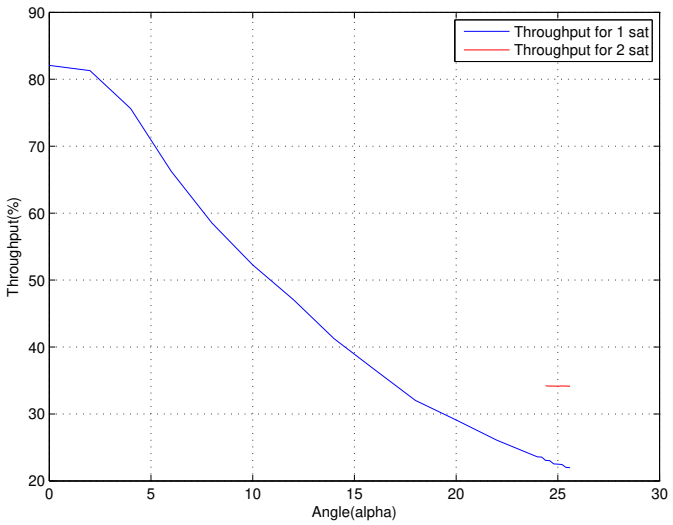

Figure 4.9: Throughput(α)

Figure 4.9 shows that once the terminal enters the handover zone, the throughput grows 10% due to the diversity gains produced by the communication with two satellites. When α reaches the middle zone (where the MT is equidistant from both satellites), the throughput difference between sending the signal for one and for two satellites, increases to a maximum value, because the largest distance on a communication with only one satellite is reached, meaning that it is in the imminence of switching the communication to the second satellite. The graph for the rest of terminal course, which is from $\alpha = \frac{\theta}{2}$ to $\alpha = \theta$, will be like a mirrored version of this throughput graphic, where the throughput increase with a similar pattern as it decreases in this figure.

4.4.4 Energy Consumption Analysis

In terms of energy consumption, figure 4.10 indicates that a gain of 3.4dBs is obtained once the terminal enters the handover zone due to the additional space diversity.

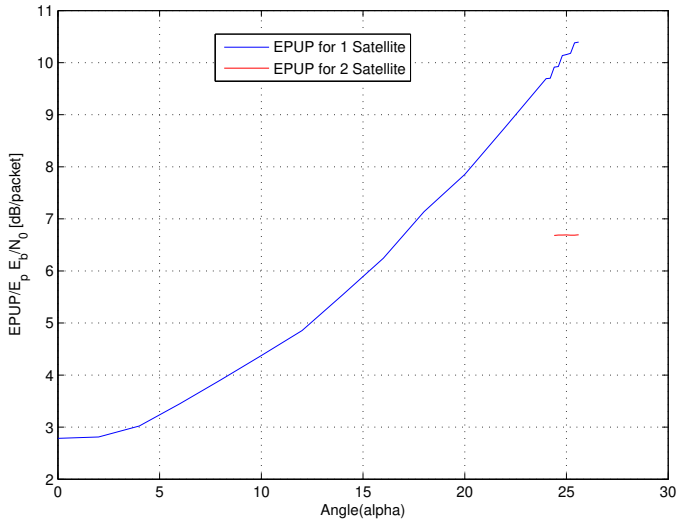

Figure 4.10: EPUP(α)

It is possible to observe in figure 4.10 that the gain resulting from the communication with two satellites increases in the handover zone, until it reaches the middle of this zone. Figure 4.10 shows only half of the handover zone, until the equidistant point for both satellites. The other half is symmetric. Although the area coverage by both satellites is short, it can be seen that the use of spatial diversity almost sets EPUP and throughput almost constant in the handover zone, where these parameters reach their critical values for an hard-handover approach.

4.4.5 Packet Delay Analysis

Figure 4.11 depicts the average packet delay over angle α variation, for a communication with a single satellite and with two satellites, using S-NDMA protocol. It takes into

account the retransmission probabilities of S-NDMA for a single satellite, and the propagation delay for the furthest satellite and the ISL for two satellites. It can be seen that average packet delay is lower when communicating with two satellites (i.e. in the handover zone). As it is possible to attend in figure 4.11, a decrease of approximately 1 ms in packet's delay is verified once the terminal enters the handover zone. The large distance between both satellites is responsible for increasing the packet delay, but in this case, the number of retransmissions when a MT is communicating with a single satellite leads to a higher packet delay. The packet's delay, δ_T, for a communication with two satellites is defined by the longest path traversed by the packet, plus the packet transmission time. For the scenario of Figure 4.1, it is calculated using $\delta_T = \delta_{MT-B} + \delta_{B-A} + (P + n_0)\delta_p$, where δ_{MT-B}, δ_{B-A} and δ_p denote respectively the propagation delay from the MT to satellite B, the propagation delay in the ISL, and the packet transmission time, which is multiplied by the number of transmitted copies.

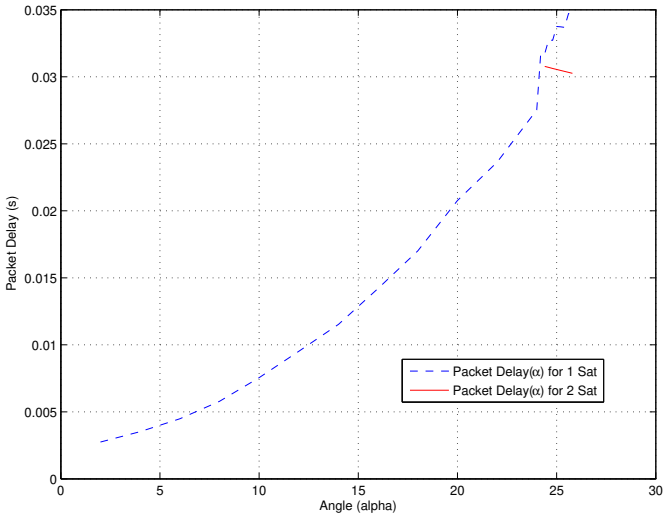

Figure 4.11: Packet Delay(α)

4.5 Iridium Handover Scheme Performance Analysis

This section presents results concerning throughput, energy consumption, packet delay, Doppler deviation and time offset, for the Iridium Handover Scheme.

4.5.1 Doppler Deviation

Just like it was approached on the last section, this Doppler deviation sub-section studies the changes on received carrier frequency, but in this case, is on the satellites of Iridium handover scheme (figure 4.5). Equation (4.4) was used in this study too, in order to calculate the value of the Doppler frequency shift.

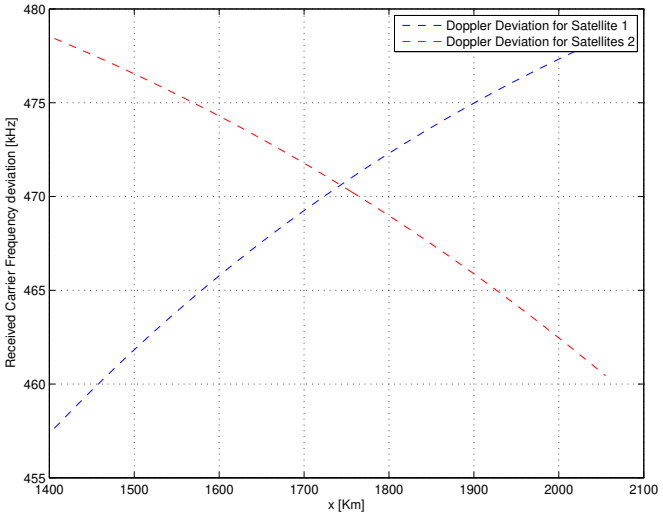

Figure 4.12: Doppler Deviation for Iridium Handover Scheme(x)

Figure 4.12 depicts the received carrier frequency deviation changes by taking into account the different MT locations, from 1406Km to 2055Km which is the interval of the handover zone, represented in figure 4.5 by the overlap of the two satellite footprints where the cellphones line crosses.

The behaviour of the Doppler shifts in figure 4.12 are similar to the ones depicted in figure 4.6, but the values of received carrier frequency deviation for Iridium handover scheme are a little bit smaller, because on this scenario, the distance between terminals and satellites is smaller. The carrier frequency is the same (2 GHz) in this scenario, and the values that are present in figure 4.12 are the deviation values relative to that original carrier frequency. It is possible to see that initially, the deviation for the first satellite is lower than the deviation for the second, who are respectively the closest and farthest satellites on the moment the MT enters the handover zone. The moment where the two line crosses ($1743km$) is when the MT is equidistant to both satellites. An almost symmetric process is done after this point, where the terminal is closer to the second satellite and farthest from the first. The approach to handle this constrain is the same as previously presented in section 4.4.1.

4.5.2 Time Offset

The time offset constrain, that was already exposed in section 4.4.2 is also analysed in this Iridium handover scheme. Figure 4.13 depicts the propagation delay between the MT communication with one and with two satellites, only in the handover zone ($x = 1406$Km to $x = 2055$Km). The CDMA data blocks size ($N = 256$ bits) and the CDMA spreading factor ($S_f = 128$) remain the same for this scenario.

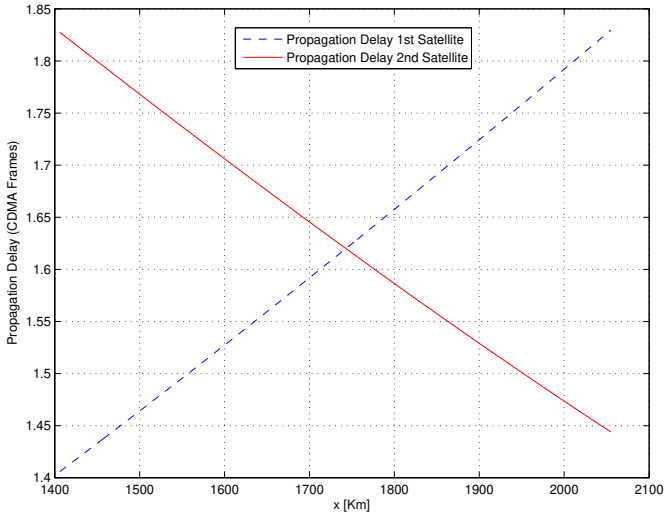

Figure 4.13: Propagation Delay (x)

Figure 4.13 shows that once the terminal enters the handover zone, there is a difference of approximately 0.42 CDMA Frames, between the closest and the furthest satellite. If the CP size is stipulated in 15% of the CDMA Frame's size, in order to gain spectral efficiency, the terminal has approximately 150 km to do the handover process, which is approximately from $x = 1670$ km to $x = 1820$ km, where the difference of data blocks is smaller than the CP. In this handover model, the satellites are closer to the MTs, so the margin to do the handover process is bigger and more slots can be allocated, so it is easier to decrease the size of the CP, improving the spectral efficiency, and it stills compensate the time offsets.

4.5.3 Throughput Analysis

Unlike the throughput analysis for the intra planar handover scheme that is made only to halfway of handover zone, the throughput analysis for the Iridium handover scheme is made for all the zone where the MT is communicating with both satellites.

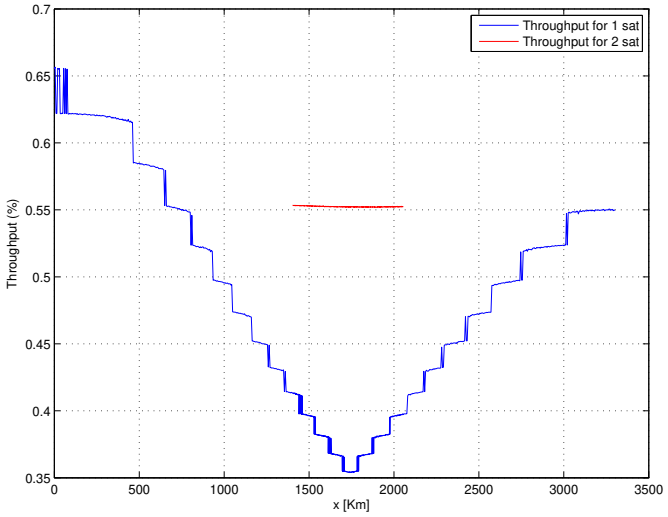

Figure 4.14: Throughput (x)

Figure 4.14 depicts the throughput values in the communication with only one satellite during the travel of a MT in an interval that goes from 0 km to 3315 km. This interval corresponds to the course of the MT, represented by the cellphones line of figure 4.5.

The red line in figure two corresponds to the throughput that results from the communication of the MT with two satellites, and the blue line represents the throughput measured with the communication with a single satellite. In figure 4.14 it can be seen that as soon as the terminal enters the handover zone (which is when the red line starts), an increase of approximately 15% on throughput is verified.

The several abrupt changes in throughput values are caused by the increase of ζ_l, which results in a larger number of copies of a packet, that occur in view of the different distance between the MT and the satellite, resulting in a growth of the NDMA complexity. This NDMA complexity increases or decreases, in order to achieve the stipulated QoS requirements minimizing the energy consumption..

The point in figure 4.14 where the difference of throughput values is greater, is the point where the terminal is equidistant to both satellites. After this point, the MT is aligned with the satellite that initially was the farthest, so the handover process occurs, and when the terminal leaves the handover zone (end of red line), it will only communicate with that satellite.

4.5.4 Energy Consumption Analysis

Figure 4.15 depicts the EPUP values for different MT locations, which goes from 0 km to 3315 km. Like it was mentioned before, it indicates the cellphones line on figure 4.5.

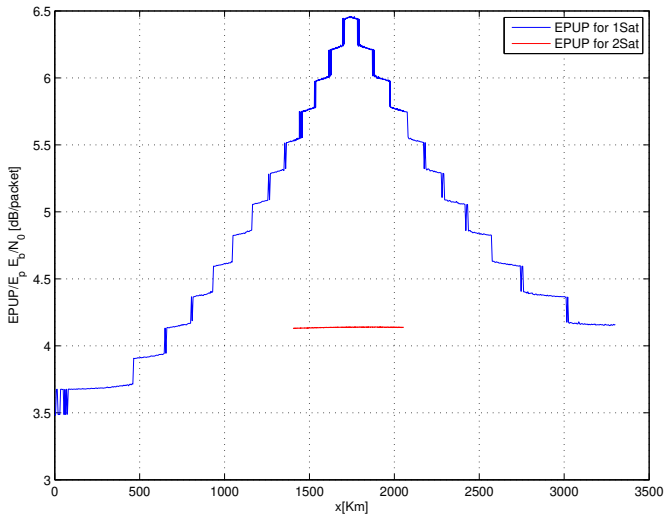

Figure 4.15: EPUP (x)

The red line represents the communication between a MT and two satellites, and the blue line the communication with a single satellite at a time. When the red line starts (1406 km), indicating the beginning of the zone where the MT is able to communicate with both satellites (handover zone), a gain of approximately 1.4dBs is verified. Initially ($x = 0$ km) the MT is at a point that has the shortest distance to the first satellite and the farthest distance to the second satellite. When the MT reaches the handover zone, it is still closer to the first satellite than the second, so the gain in this stage is the minimum in the handover zone (1.4dBs). The gain grows until the terminal reaches the kilometre 1743, where it is equidistant to both satellites, and needs the maximum EPUP to communicate with only one of them. In this situation, the gain to the communication with two satellites at the same time is maximum (approximately 2.3 dBs) . The gain decreases after this point, until it leaves the handover zone, because the terminal is getting closer to the second satellite and the EPUP for the communication with only the second satellite is decreasing too.

Once again, it is visible the effect of spatial diversity on energy consumption, because it makes EPUP almost constant during the handover process, due to the approximately constant ζ_l throughout the roam of MT in the handover zone.

4.5.5 Packet Delay Analysis

Figure 4.16 depicts the average packet delay over the x axis represented in figure 4.5 by the cellphones line. As it was said before, the packet delay involves the retransmission probabilities of S-NDMA for a single satellite and the propagation delay for the furthest satellite and ISL between the two satellites.

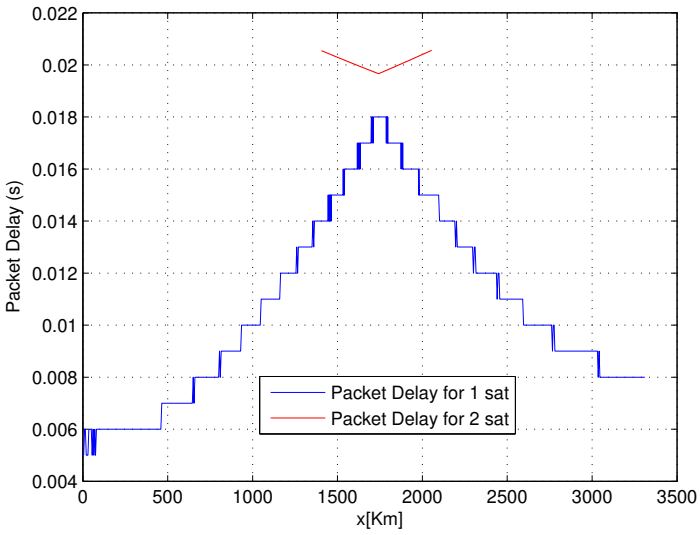

Figure 4.16: Packet Delay(x)

As soon as the MT enters the handover zone, the communication with both satellites leads to an increase of approximately 6 ms the packet delay, and in the point where the MT reaches the point $x = 1743$ km (point equidistant to both satellites), it has a maximum difference of 1.8 ms. The fact that the communication with two satellites does not have retransmissions is an advantage, but it is not sufficient to have a lower packet delay, because the packet delay is very influenced by the large distance between satellites. The difference is not significant, but in this case the packet delay is higher for the communication with two satellites, due to the lowest satellites' altitude for this scenario.

5

Conclusions and Future Work

During this dissertation a new NDMA protocol was proposed, S-NDMA, that can be regarded as a H-NDMA protocol especially designed to provide QoS guarantees for scenarios with a high RTT, such as a satellite network. An analytical model was derived for the network throughput, energy consumption and packet delay for S-NDMA. A configuration method was also proposed to configure S-NDMA to provide a given QoS level. The S-NDMA performance was compared to H-NDMA, showing that a properly configured S-NDMA system is capable of satisfying the QoS constraints of the video telephony traffic with only a slight degradation on the energy efficiency of H-NDMA. Therefore, it can be a good option for the satellite links of future high data rate hybrid satellite-cellular networks.

The S-NDMA was used to handle two satellite handover schemes, and it was proved to be efficient in terms of energy consumption and throughput, satisfying the QoS requirements. The handover process benefits from spatial diversity, and it was showed that its existence improved the energy consumption and throughput, but introduces constraints of Doppler deviation and time offset and packet delay (in the Iridium scheme case). This dissertation has provided solutions for those issues. It also proposed the use of CDMA with NDMA to limit the calculation complexity, and it was possible to verify that this solution can handle the low power that mobile terminals use to communicate with satellites, by spreading the bandwidth and decrease the noise power. Although the data rate is reduced.

In terms of future work, it would be interesting to apply satellite diversity for higher orbits, for instance MEO satellites. New satellite constellations could be designed, providing the existence of more overlapping among satellite footprints and specially suited to handle time offset and Doppler deviation constraints, where the capacities of SIMO

S-NDMA can be exploited.
Another challenge that can be approached for future work is to increase the data rate in the communications between the mobile terminals and satellites. A possible approach to improve data rate is by using coded transmissions (e.g. turbo codes), in order to take full advantage of channel capacities.

Bibliography

[Abr92] N. Abramson. Fundamentals of packet multiple access for satellite networks. *IEEE Journal on Selected Areas in Communications*, Vol.10(No.2):pages 309–316, Feb 1992.

[AM96] A. Azzarelli and R. Manohar. Visibility of non-gso satellites from a terrestrial station and applications to inter-system interference. In *Fifth International Conference on Satellite Systems for Mobile Communications and Navigation, 1996*, pages 106–109, May 1996.

[AMCV06] N. Anastacio, F. Merca, O. Cabral, and F.J. Velez. Qos metrics for cross-layer design and network planning for b3g systems. In *3rd International Symposium on Wireless Communication Systems, 2006. (ISWCS '06.)*, pages 592 –596, Sept. 2006.

[AMGL10] S. Arnold, G. Montgomery, R. Gopal, and D. Losada. Validation of high-speed broadband satellite communications on airborne platforms. In *Military Communications Conference, 2010 - MILCOM 2010*, pages 2003 –2008, Nov 2010.

[ASL00] O. Ait Sab and V. Lemaire. Block turbo code performances for long-haul dwdm optical transmission systems. In *Optical Fiber Communication Conference*, volume 3, pages 280–282, 2000.

[BCW96] R.M. Buehrer, N.S. Correal, and B.D. Woerner. A comparison of multiuser receivers for cellular cdma. In *Global Telecommunications Conference, 1996. (GLOBECOM '96.)*, volume 3, pages 1571 –1577, Nov 1996.

[BFC05] Daniel W. Bliss, Keith W. Forsythe, and Amanda M. Chan. Mimo wireless communication. *Lincoln Laboratory Journal*, Vol.15(No.1):pages 97–126, 2005.

[BNNK08] A.M. Baker, Chee Kyun Ng, N.K. Noordin, and S. Khatun. Phy and mac, cross-layer optimization and design. In *6th National Conference on Telecommunication Technologies 2008 and 2008 2nd Malaysia Conference on Photonics. (NCTT-MCP 2008.)*, pages 192 –197, Aug. 2008.

[BWZ00] D.J. Bem, T.W. Wieckowski, and R.J. Zielinski. Broadband satellite systems. *IEEE Communications Surveys Tutorials*, Vol.3(No.1):pages 2–15, quarter 2000.

[CAI06a] P.K. Chowdhury, M. Atiquzzaman, and W. Ivancic. Handover schemes in satellite networks: state-of-the-art and future research directions. *IEEE Communications Surveys Tutorials*, Vol.8(No.4):pages 2–14, Nov. 2006.

[CAI06b] P.K. Chowdhury, M. Atiquzzaman, and W. Ivancic. Handover schemes in space networks: classification and performance comparison. In *Second IEEE International Conference on Space Mission Challenges for Information Technology, 2006. (SMC-IT 2006.)*, pages 8–108, Nov 2006.

[CC84] R. Comroe and Jr. Costello, D. ARQ schemes for data transmission in mobile radio systems. *IEEE Journal onSelected Areas in Communications*, Vol.2(No.4):pages 472 –481, July 1984.

[CLZ08] P. Casari, M. Levorato, and M. Zorzi. MAC/PHY cross-layer design of mimo ad hoc networks with layered multiuser detection. *IEEE Transactions on Wireless Communications*, Vol.7(No.11):pages 4596–4607, November 2008.

[CY99] P. Chitre and F. Yegenoglu. Next-generation satellite networks: architectures and implementations. *IEEE Communications Magazine*, Vol.37(No.3):pages 30 –36, Mar 1999.

[DMB+09] R. Dinis, P. Montezuma, L. Bernardo, R. Oliveira, M. Pereira, and P. Pinto. Frequency-domain multipacket detection: a high throughput technique for sc-fde systems. *IEEE Transactions on Wireless Communications*, Vol.8(No.7):pages 3798–3807, July 2009.

[FABSE02] D. Falconer, S.L. Ariyavisitakul, A. Benyamin-Seeyar, and B. Eidson. Frequency domain equalization for single-carrier broadband wireless systems. *IEEE Communications Magazine*, Vol.40(No.4):pages 58–66, Apr 2002.

[FC07] G.D. Forney and D.J. Costello. Channel coding: The road to channel capacity. *Proceedings of the IEEE*, Vol.95(No.6):pages 1150–1177, June 2007.

[Fel96] Phillip M. Feldman. *An Overview and Comparison of Demand Assignment Multiple Access (DAMA) Concepts for Satellite Communications Networks*. RAND Corporation, 1996.

[GDB+11] Francisco Ganhão, Rui Dinis, Luis Bernardo, Paulo Carvalho, Rodolfo Oliveira, and Paulo Pinto. Analytical performance evaluation of sc-fde modulations with packet combining and multipacket detection schemes. In *VTC Spring'11*, pages 1–5, 2011.

[GKVW04] P. Gupta, G. Kramer, and A.J. Van Wijngaarden. *Advances In Network Information Theory: Dimacs Workshop Network Information Theory, March 17-19, 2003, Piscataway, New Jersey*. DIMACS Series in Discrete Mathematics and Theoretical Computer Science. American Mathematical Society, 2004.

[GLASW07] J. J. Garcia-Luna-Aceves, Hamid R. Sadjadpour, and Zheng Wang. Challenges: towards truly scalable ad hoc networks. In *Proceedings of the 13th annual ACM international conference on Mobile computing and networking*, MobiCom '07, pages 207–214, New York, NY, USA, 2007. ACM.

[GPB+11] Francisco Ganhão, Miguel Pereira, Luis Bernardo, Rui Dinis, Rodolfo Oliveira, and Paulo Pinto. Performance of hybrid arq for ndma access schemes with uniform average power control. *Journal of Communications*, Vol.6(No.9), 2011.

[HKL97] Bruce Hajek, Arvind Krishna, and Richard O. Lamaire. On the capture probability for a large number of stations. *IEEE Transactions on Communications*, Vol.45:pages 254–260, 1997.

[HLZ08] Wei Lan Huang, K. Letaief, and Ying Jun Zhang. Cross-layer multi-packet reception based medium access control and resource allocation for space-time coded mimo/ofdm. *IEEE Transactions on Wireless Communications*, Vol.7(No.92):3372 –3384, September 2008.

[Jos06] Lars Josefsson. *Conformal Array Antenna Theory and Design*. Wiley-IEEE Press, first edition, 2006.

[Jr.08] Louis J. Ippolito Jr. *Satellite Communications Systems Engineering: Atmospheric Effects, Satellite Link Design and System Performance (Wireless Communications and Mobile Computing)*. Wiley, first edition, 2008.

[KR09] James Kurose and Keith Ross. *Computer Networking: A Top-Down Approach (5th Edition)*. Addison-Wesley, fifth edition, 2009.

[KRT11] K.Supraja, A. Srinivasa Reddy, and R. Lakshmi Tulasi. Evaluating efficacy of forward error correction coding. *International Journal of Computer Trends and Technology*, pages 187–194, August 2011.

[LC83] Shu Lin and D.J. Costello. *Error control coding: fundamentals and applications*. Prentice-Hall computer applications in electrical engineering series. Prentice-Hall, 1983.

[LCM84] Shu Lin, D. Costello, and M. Miller. Automatic-repeat-request error-control schemes. *IEEE Communications Magazine*, Vol.22(No.12):pages 5–17, December 1984.

[LSW12] Jia-Liang Lu, Wei Shu, and Min-You Wu. A survey on multipacket reception for wireless random access networks. *Journal of Computer Networks and Communications*, 2012.

[LV90] R. Lupas and S. Verdu. Near-far resistance of multiuser detectors in asynchronous channels. *IEEE Transactions on Communications*, Vol.38(No.4):pages 496 –508, Apr 1990.

[MAEIB12] Amr S. Matar, Gamal Abd-Elfadeel, Ibrahim I. Ibrahim, and Hesham M. Z. Badr. Handover priority schemes for multi-class traffic in leo mobile satellite systems. *IJCSI International Journal of Computer Science Issues*, Vol.9(No.1), January 2012.

[Miz06] T. Mizuochi. Recent progress in forward error correction and its interplay with transmission impairments. *IEEE Journal of Selected Topics in Quantum Electronics*, Vol.12(No.4):pages 544–554, July-Aug. 2006.

[Miz09] T. Mizuochi. Forward error correction in next generation optical communication systems. In *Conference on Quantum electronics and Laser Science Conference Lasers and Electro-Optics, 2009 and 2009. CLEO/QELS 2009. Conference on*, June 2009.

[NBSL11] N. Natarajan, A. Bagchi, W.E. Stephens, and S.J. Leanheart. Network architecture for mission critical communications using leo satellites. In *Military Communications Conference, 2011 - MILCOM 2011*, Nov. 2011.

[Ngu02] Hoang Nam Nguyen. *Routing and Quality-of-Service in Broadband LEO Satellite Networks (Broadband Networks and Services)*. Springer, first edition, 2002.

[NLSvA01] Hoang Nam Nguyen, S. Lepaja, J. Schuringa, and H.R. van As. Handover management in low earth orbit satellite ip networks. In *IEEE Global Telecommunications Conference, (GLOBECOM '01.)*, volume 4, pages 2730–2734, 2001.

[OLLMML03] A.G. Orozco-Lugo, M.M. Lara, D.C. McLernon, and H.J. Muro-Lemus. Multiple packet reception in wireless ad hoc networks using polynomial phase-modulating sequences. *IEEE Transactions on Signal Processing*, Vol.51(No.8):pages 2093–2110, Aug. 2003.

[O'R89] J. O'Reilly. *Telecommunications Principles*. Tutorial Guides in Electronic Engineering. Springer, 1989.

[PA02] Ernesto Pinto and Claudio Albuquerque. A técnica de transmissão OFDM. *Revista Científica Periódica*, 2002.

[Pet07] Larry L. Peterson. *Computer Networks: A Systems Approach*. Morgan Kaufmann, fourth edition, 2007.

[Pey99] H. Peyravi. Medium access control protocols performance in satellite communications. *Communications Magazine, IEEE*, Vol.37(No.3):pages 62–71, Mar 1999.

[PRFT99] S.R. Pratt, R.A. Raines, C.E. Fossa, and M.A. Temple. An operational and performance overview of the IRIDIUM low earth orbit satellite system. *IEEE Communications Surveys Tutorials*, Vol.2(No.2):pages 2–10, quarter 1999.

[Rap09] Rappaport. *Wireless Communications: Principles and Practice*. Pearson Education, 2009.

[Ret80] C. Retnadhas. Satellite multiple access protocols. *IEEE Communications Magazine*, Vol.18(No.5):pages 16–20, September 1980.

[RP12] Ramya.R and Padmapriya.S. Multi packet reception technique with mimo assisted cross layered mac/phy algorithm over a jittery channel. *International Journal of Research in Communication Technologies- IJRCT*, Vol.1(No.1), 2012.

[SA05] A.Goldsmith S.Cui and A.Bahai. Energy-constrained modulation optimization. *IEEE Transactions on Wireless Communications*, Vol.4(No.5):pages 2349–2360, Sept. 2005.

[Sha48] C.E. Shannon. A mathematical theory of communication. *The Bell System Technical Journal*, Vol.27:pages 379–423, 1948.

[SY07] Ryutaro Suzuki and Yasuhiko Yasuda. Study on isl network structure in leo satellite communication systems. *Acta Astronautica*, Vol.61(No.(7–8)):pages 648 – 658, 2007.

[Tan02] Andrew S. Tanenbaum. *Computer Networks*. Prentice Hall, 2002.

[TZB98] M.K. Tsatsanis, Ruifeng Zhang, and S. Banerjee. Network assisted diversity for random access wireless data networks. In *Conference Record of the Thirty-Second Asilomar Conference on Signals, Systems amp; Computers*, volume 1, pages 83–87, Nov. 1998.

[TZB00] M.K. Tsatsanis, Ruifeng Zhang, and S. Banerjee. Network-assisted diversity for random access wireless networks. *IEEE Transactions on Signal Processing*, Vol.48(No.3):pages 702 –711, Mar 2000.

[vdVT02] Alle-Jan van der Veen and Lang Tong. Packet separation in wireless ad-hoc networks by known modulus algorithms. In *IEEE International Conference on Acoustics, Speech, and Signal Processing (ICASSP)*, volume 3, pages III–2149 –III–2152, May 2002.

[WFGV98] P.W. Wolniansky, G.J. Foschini, G.D. Golden, and R.A. Valenzuela. V-blast: an architecture for realizing very high data rates over the rich-scattering wireless channel. In *URSI International Symposium on Signals, Systems, and Electronics (ISSSE 98) 1998*, pages 295–300, Sep-Oct 1998.

[WGLA09] Xin Wang and J. J. Garcia-Luna-Aceves. Embracing interference in ad hoc networks using joint routing and scheduling with multiple packet reception. *Ad Hoc Netw.*, Vol.7(No.2):460–471, Mar 2009.

[Wic94] Stephen B. Wicker. *Error Control Systems for Digital Communication and Storage*. Prentice-Hall, US edition, 1994.

[WSGLA08] Zheng Wang, Hamid Sadjadpour, and Jose Joaquin Garcia-Luna-Aceves. The capacity and energy efficiency of wireless ad hoc networks with multi-packet reception. In *Proceedings of the 9th ACM international symposium on Mobile ad hoc networking and computing*, MobiHoc '08, pages 179–188, New York, NY, USA, 2008. ACM.

[www10] www.iridium.com. The global network: The satellite constellation, 2010.

[ZCM12] Xiaohui Zhang, Enqing Chen, and Xiaomin Mu. Single-carrier frequency-domain equalization based on frequency-domain oversampling. *IEEE Communications Letters*, Vol.16(No.1):24 –26, january 2012.

[ZR94] M. Zorzi and R.R. Rao. Capture and retransmission control in mobile radio. *IEEE Journal on Selected Areas in Communications*, Vol.12(No.8):pages 1289 –1298, Oct 1994.

[ZST02] Ruifeng Zhang, N.D. Sidiropoulos, and M.K. Tsatsanis. Collision resolution in packet radio networks using rotational invariance techniques. *IEEE Transactions on Communications*, Vol.502(No.1):pages 146–155, Jan 2002.

[ZT02] Ruifeng Zhang and M.K. Tsatsanis. Network-assisted diversity multiple access in dispersive channels. *IEEE Transactions on Communications*, Vol.50(No.4):pages 623–632, Apr 2002.

[ZZL06] Peng Xuan Zheng, Ying Jun Zhang, and Soung Chang Liew. Multipacket reception in wireless local area networks. In *IEEE International Conference on Communications, (2006. ICC '06.)*, volume 8, pages 3670–3675, June 2006.